NASA/TM–2012-217784
NESC-RP-10-00632

Icing Research Tunnel (IRT) Force Measurement System (FMS)

Paul W. Roberts/NESC
Langley Research Center, Hampton, Virginia

November 2012

NASA STI Program . . . in Profile

Since its founding, NASA has been dedicated to the advancement of aeronautics and space science. The NASA scientific and technical information (STI) program plays a key part in helping NASA maintain this important role.

The NASA STI program operates under the auspices of the Agency Chief Information Officer. It collects, organizes, provides for archiving, and disseminates NASA's STI. The NASA STI program provides access to the NASA Aeronautics and Space Database and its public interface, the NASA Technical Report Server, thus providing one of the largest collections of aeronautical and space science STI in the world. Results are published in both non-NASA channels and by NASA in the NASA STI Report Series, which includes the following report types:

- TECHNICAL PUBLICATION. Reports of completed research or a major significant phase of research that present the results of NASA Programs and include extensive data or theoretical analysis. Includes compilations of significant scientific and technical data and information deemed to be of continuing reference value. NASA counterpart of peer-reviewed formal professional papers, but having less stringent limitations on manuscript length and extent of graphic presentations.

- TECHNICAL MEMORANDUM. Scientific and technical findings that are preliminary or of specialized interest, e.g., quick release reports, working papers, and bibliographies that contain minimal annotation. Does not contain extensive analysis.

- CONTRACTOR REPORT. Scientific and technical findings by NASA-sponsored contractors and grantees.

- CONFERENCE PUBLICATION. Collected papers from scientific and technical conferences, symposia, seminars, or other meetings sponsored or co-sponsored by NASA.

- SPECIAL PUBLICATION. Scientific, technical, or historical information from NASA programs, projects, and missions, often concerned with subjects having substantial public interest.

- TECHNICAL TRANSLATION. English-language translations of foreign scientific and technical material pertinent to NASA's mission.

Specialized services also include organizing and publishing research results, distributing specialized research announcements and feeds, providing information desk and personal search support, and enabling data exchange services.

For more information about the NASA STI program, see the following:

- Access the NASA STI program home page at *http://www.sti.nasa.gov*

- E-mail your question to help@sti.nasa.gov

- Fax your question to the NASA STI Information Desk at 443-757-5803

- Phone the NASA STI Information Desk at 443-757-5802

- Write to:
  STI Information Desk
  NASA Center for AeroSpace Information
  7115 Standard Drive
  Hanover, MD 21076-1320

NASA/TM–2012-217784
NESC-RP-10-00632

Icing Research Tunnel (IRT) Force Measurement System (FMS)

Paul W. Roberts/NESC
Langley Research Center, Hampton, Virginia

National Aeronautics and
Space Administration

Langley Research Center
Hampton, Virginia 23681-2199

November 2012

Available from:

NASA Center for AeroSpace Information
7115 Standard Drive
Hanover, MD 21076-1320
443-757-5802

Icing Research Tunnel (IRT) Force Measurement System (FMS)

September 20, 2012

NESC Request No.: TI-10-00632

Approval and Document Revision History

NOTE: This document was approved at the September 20, 2012, NRB. This document was submitted to the NESC Director on October 1, 2012, for configuration control.

Approved:	*Original Signature on File*	10/2/12
	NESC Director	Date

Version	Description of Revision	Office of Primary Responsibility	Effective Date
1.0	Initial Release	Mr. Paul Roberts, NESC Associate Principal Engineer	9/20/12

Table of Contents

Technical Assessment Report

List of Figures

List of Tables

Technical Assessment Report

1.0 Notification and Authorization

Mr. Mark Woike, Electronics Engineer at the Glenn Research Center (GRC), requested that the NASA Engineering and Safety Center (NESC) provide technical support for an evaluation of the existing force measurement system (FMS) at the GRC's Icing Research Tunnel (IRT) with the intent of developing conceptual designs to improve the tunnel's force measurement capability in order to better meet test customer needs.

An NESC initial evaluation was approved on October 1, 2010. Mr. Paul Roberts, NESC Associate Principal Engineer at Langley Research Center (LaRC), was assigned to lead the assessment. An Assessment Plan was approved by the NESC Review Board (NRB) on July 29, 2010.

The key stakeholder for this assessment was Mr. Mark Woike at GRC.

2.0 Signature Page

Submitted by:

Team Signature Page on File – 10/4/12

Mr. Paul W. Roberts Date

Significant Contributors:

Mr. Ray D. Rhew Date

Mr. Jared A. Dervan Date

Dr. Drew Landman Date

Mr. K. Christopher Lynn Date

Mr. Nans Kunz Date

Mr. David King Date

Mr. Naresh Patel Date

Signatories declare the findings, observations, and NESC recommendations compiled in the report are factually based from data extracted from Program/Project documents, contractor reports, and open literature, and/or generated from independently conducted tests, analyses, and inspections.

3.0 Team List

Name	Discipline	Organization/Location
Core Team		
Paul Roberts	NESC Team Lead, Associate Principal Engineer	LaRC
Ray Rhew	FMS Engineer – Deputy	LaRC
Jared Dervan	Resident Engineer	MSFC
David King	FMS Engineer	Triumph Aerospace
Nans Kunz	NESC Chief Engineer	ARC
Drew Landman	Statistics	Old Dominion University
Chris Lynn	FMS Engineer	LaRC
Naresh Patel	FMS Engineer	Modern Machine & Tool
Roy Savage	MTSO Program Analyst	LaRC
Mark Woike	Electronics Engineer	GRC
Administrative Support		
Linda Burgess	Planning and Control Analyst	LaRC/AMA
Tina Dunn-Pittman	Project Coordinator	LaRC/AMA
Christina Williams	Technical Writer	LaRC/AMA

4.0 Executive Summary

The Glenn Research Center (GRC) Icing Research Tunnel (IRT) is one of NASA's unique aerodynamic test facilities. It is one of the largest icing wind tunnels in the world. Because of this unique capability, the facility is constantly in high demand. Some of the tunnel's main features are a large external balance and turntable system. The IRT is considering upgrades to these systems to increase the force and moment measurement accuracy and to improve facility test throughput. This force measurement system (FMS) was designed in the early 1970s by civil servants who have since retired. The IRT operations crew is considering options to improve their facility product quality, reliability, and test throughput. To support this effort, the NASA Engineering and Safety Center (NESC) was requested to assess the current system, evaluate operational needs, and develop new concepts and/or upgrade options including the associated cost estimates.

The NESC created a team of experts from across NASA and industry to perform this assessment. This involved becoming familiar with the existing facility and interviewing the operations staff to gain an understanding of current operations and facility weaknesses and to solicit their thoughts on requirements, needs, goals, and desires. The NESC team then developed multiple design configuration upgrade options that would meet these requirements/needs/goals. The pros and cons of each system were first discussed within the team, and then the first round of down selected concepts was discussed with the facility personnel. The pros and cons, expected accuracy, benefits, etc., for each of the final down selected options are discussed in this report. As part of this assessment, the NESC team performed a system uncertainty analysis to compare the current system accuracies with predicted accuracies of various upgrade concepts. A structural evaluation was included as well to gain a high confidence in the ability to upgrade the existing facility.

Since it is unknown how much funding would be ultimately available to upgrade this facility, the resulting recommendations include upgrade design concepts/options at different cost levels. The NESC recommendations to the IRT range from lower cost options including using the current hardware and changing the current calibration method to higher cost options that include replacing the entire turntable and the FMS. The benefits for each of these recommended options should help the facility determine which upgrades will have the most impact relative to their available funding. The specifications/descriptions in this report can also be used to help develop the statement of work, specifications, and other documentation that will be needed to begin the IRT modification/upgrade project.

5.0 Assessment Plan

The IRT at GRC has a complex multi-piece force measurement and turntable system that is expected to need upgrades in the near future. There are few force measurement experts in the United States or in the world that have experience with these types of systems. The scope of this task included performing an assessment of the current IRT FMS, developing concepts for improvements or a new design, and generating a cost estimate and specifications that will be used to procure a new FMS.

The plan required the team to review the existing literature and other documentation of the current IRT FMS, inspect the facility, and interview the operations staff. The NESC team relied on the broad expertise of the facility personnel to become familiar with operational issues and to identify areas where the greatest potential for system improvements exists. From these interviews, a list of facility needs was developed and priorities were ranked and listed, as shown in Table 7.1-1. Following the accomplishment of these tasks, an uncertainty analysis was performed for the FMS options. Tests such as measurement of the turntable system accuracies were performed to generate the required data to complete the uncertainty analysis. Clear definition of the requirements and the development of a facility prioritization list was the next step in the process, followed by the development of multiple new system concepts. Computer-aided design models were developed, and predicted system uncertainties were calculated. The pros and cons of each concept were then discussed with the IRT facility personnel, and their thoughts were recorded. All of this information was used to down select a final recommended new system that best met all of the facility requirements. Finally, the team broke down the upgrade into possible steps and developed cost estimates and specifications such that the facility could upgrade their current system as funding becomes available.

Disengagement will occur upon the delivery of a final report describing the current FMS analysis and conceptual design improvements for upgrading the balance system. This report will include technical specifications that would allow GRC to develop a request for proposal for developing an updated FMS for the IRT.

6.0 Problem Description and Proposed Solutions

6.1 Problem Description/Current System Challenges

The GRC IRT is one of NASA's unique aerodynamic test facilities and is one of the largest icing wind tunnels in the world. Because of this unique capability, the facility is constantly in high demand. Two of the tunnel's main features that are the primary focus of this assessment are a large external balance/FMS and a turntable system.

A good representation of the entire system can be seen in the schematic of the turntable and the FMS in Figure 6.1-1.

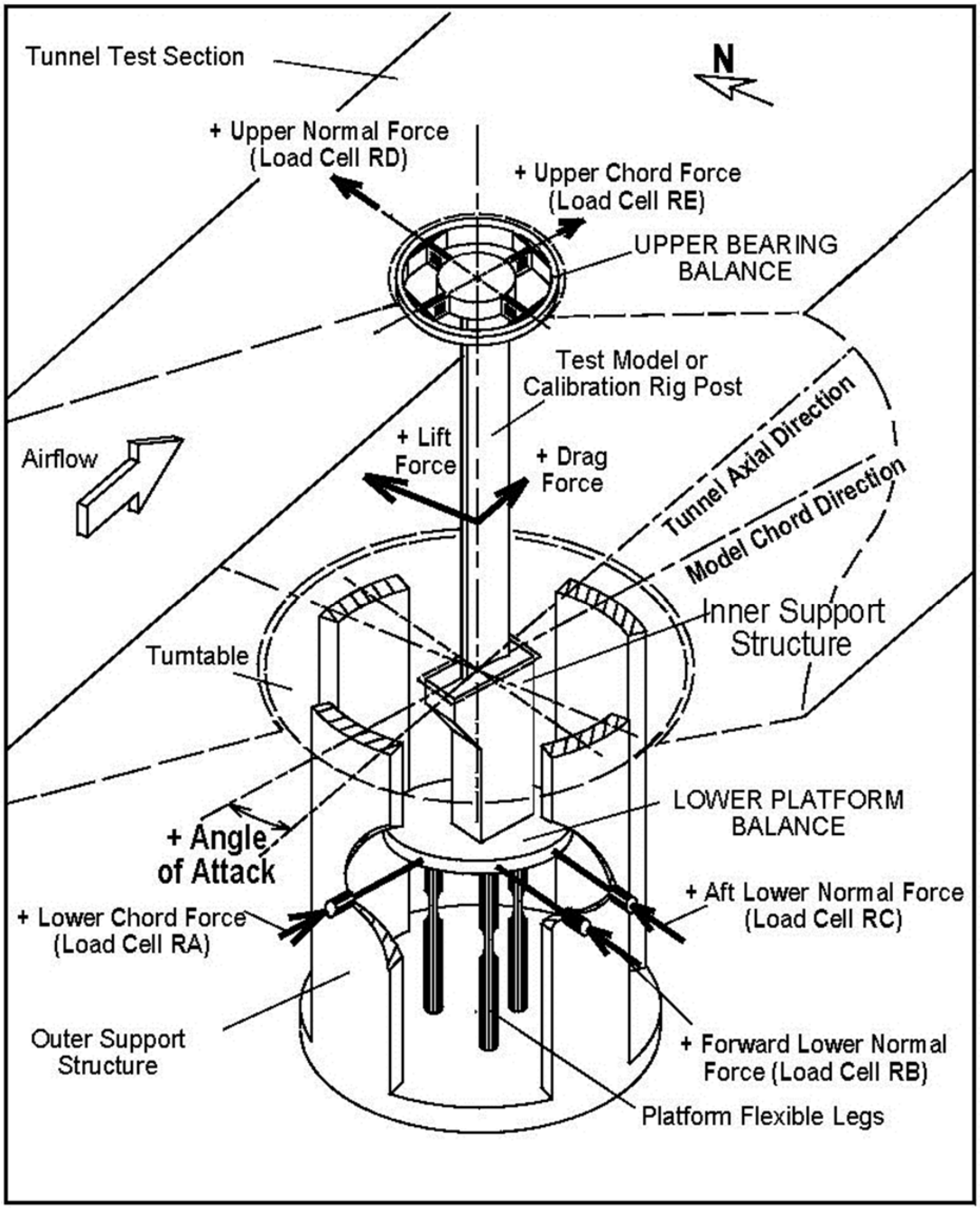

Figure 6.1-1. Schematic of the IRT FMS

Figure 6.1-2 shows some of the turntable drive system and two of the lower balance system load cell/flexure linkages. Figure 6.1-3 shows the IRT test section with the full-span calibration hardware in place. A significant amount of time and effort is required to install and remove this hardware prior to performing a calibration. As a result, the team was told that many IRT customers chose not to have the FMS in place during their tests because of the impact on productivity.

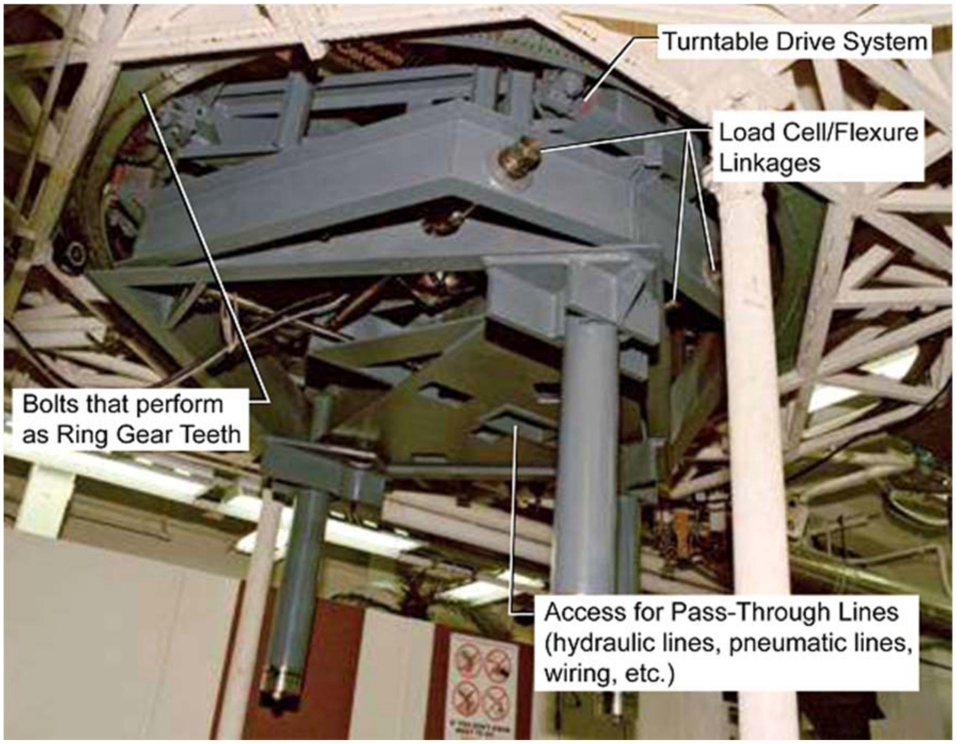

Figure 6.1-2. Lower Balance and Turntable System Directly Below the IRT Test Section

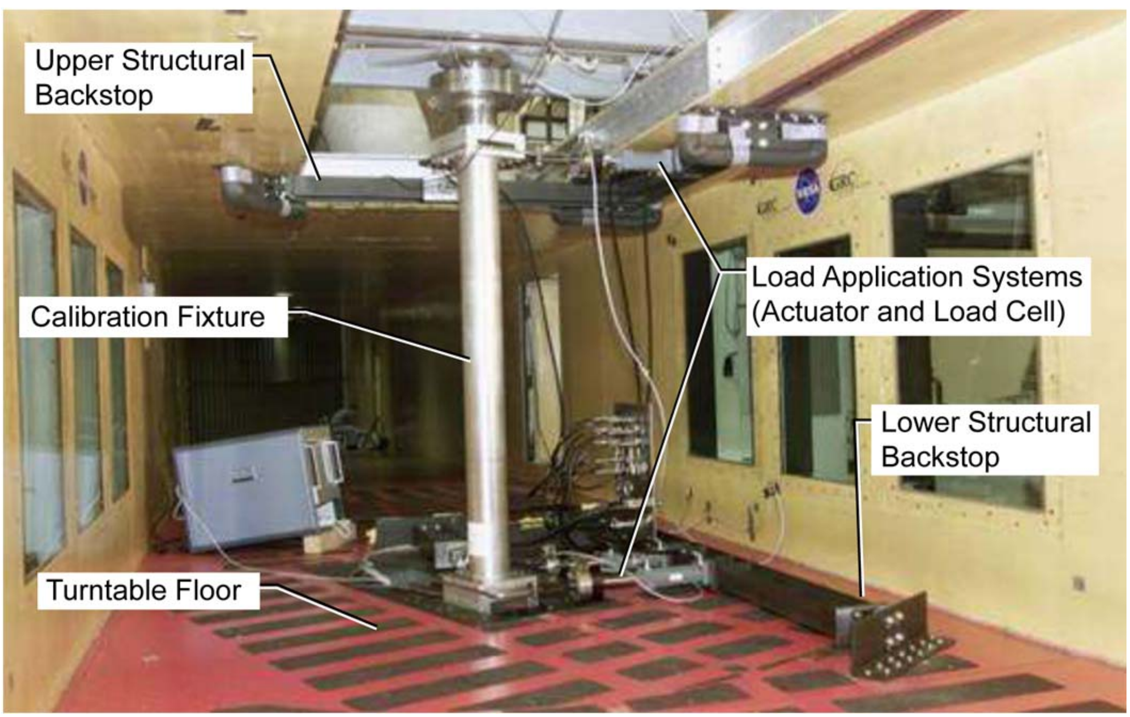

Figure 6.1-3. IRT Test Section with the Full-span Calibration Fixture Installed

A more detailed description of the current IRT force balance system can be acquired from the document, which is included in Appendix B. This system needs to be updated to increase the force and moment measurement accuracy and to improve facility throughput. From the documentation, it appears that the current FMS was last modified/updated/designed in the early 1970s by civil servants who have since retired. The NESC was requested to form a team of experts to assess the current system, develop new concepts if required, and develop cost estimates and specifications for any suggested upgrades.

6.2 IRT System Update Requests and Improvement Priorities

Through multiple meetings with the IRT team, a list of requirements, needs, requests, goals, and various background statements was generated. The list is as follows:

1. The lower balance system shall be integrated into the model turntable that will be in the IRT floor and shall replace the existing turntable system.
2. The range of the turntable shall be +/–30 degrees for model angle of attack (AOA).
3. The turntable measurement system of the AOA shall be within +/–0.05 degrees.
4. The force balance system shall measure model lift, drag, and pitching moment.
5. The maximum load measurement capability for semi-span or full-span testing shall be:
   a. 20,000 pounds lift
   b. 5,000 pounds drag
   c. 20,000 foot-pounds pitching moment
6. The loads shall be measured within +/–1 percent of full scale.
7. The force balance system should consider including an internal calibration system so no loads are required to be applied inside the test section.
8. The upper measurement system shall be integrated into the ceiling hatch with a 2-inch diameter access for instrumentation. The upper balance system can be a permanent fixture of the ceiling hatch or can be removable. The removable system would be preferred, yielding less chance for damage when not in use.
9. The upper balance system shall be used for full-span models that are attached to the turntable measurement system.
10. The design of the turntable and upper balance system must allow for thermal contraction and expansion to accommodate model length changes.
11. The turntable measurement system shall be able to withstand moisture from the cleaning of models and warm-up of the facility; water drips onto the turntable system.
12. The access area up through the balance and turntable will be 12 inches wide by 24 inches in the flow direction; the centered vertical axis will be in the center of the area (this area is for instrumentation and heated air line supply).

It is important to note that initial discussions clearly indicate that the throughput and test efficiency are potentially more important than increasing the accuracy of the FMS. Complex models that include multiple pass-through lines (e.g., high pressure air, hydraulics) are often installed in this facility. The current balance and turntable system has limited clearances for model access, which makes it challenging to install pass-through lines and keep them from fouling. Fouling lines carry loads that can introduce significant errors into the FMS. When incorporating a model pass-through, it is best to incorporate long "soft" lines paralleling the balance system. This way, the balance system carries the majority of the loads as it is designed to do. Also, it is good practice to apply the maximum loads on the model that are expected in a wind tunnel test to gain a high confidence of the system uncertainties and to check any pass-through for unacceptable fouling. Developing a system with adequate pass-through clearances and easy application of check loads will significantly increase wind tunnel productivity. Testing efficiency is a critical aspect of meeting the heavy demand for test time in this specialized wind tunnel.

6.3 Overall Current System Accuracy from the Uncertainty Analysis

During this assessment, an uncertainty analysis of the calculated aerodynamic coefficients was performed to understand the level of impact that force measurement improvements would have on the wind tunnel output data. A detailed explanation of this analysis is provided in Section 7.3. The percent error is determined by comparing the nominal coefficient value as determined by a typical semi-span icing model to the calculated systematic uncertainty. The systematic error in the aerodynamic coefficients is a function of load cell readings, the dynamic pressure, and the AOA as related through the balance data reduction equation. The equation is derived in Sections 7.3.1.4 and 7.3.1.5. The existing systematic error estimates for these parameters were researched and used in the uncertainty estimate. Existing systematic uncertainty data could be found for all sources except the turntable positioning accuracy. A test to measure the unloaded positioning accuracy was developed and performed to acquire the required data and include it in the uncertainty analysis; see Appendix C, Tables C-1 through C-3. The overall current system accuracy for a typical semi-span wing test was determined to be as follows (see Table 6.3-1).

Table 6.3-1. Current System Aerodynamic Coefficient Systematic Errors

	C_D	C_L	C_m
Total Systematic	0.005	0.023	0.024
Nominal Coefficient Value	0.147	1.02	–0.083
% of Nominal	3.54	2.32	28.3

These values do not include random error and are calculated at a 95-percent confidence level. It should be noted that a complete uncertainty analysis would include random error, which is best determined by using replicate wind tunnel test data. Unfortunately, the data were unavailable to the team.

In addition, it should be noted that the individual load cell calibration sheets supplied appear to report error well in excess of what can be inferred from the supplied whole-system calibration results. Since the pitching moment is derived from multiple load cells, it is the most affected measurement.

6.4 Concept Development and Concept Selection

Following the data-gathering phase of this assessment, the team held brainstorming sessions to develop various concepts that would improve the wind tunnel throughput and the system force measurement accuracies. It was found that the vast majority of the IRT tests are run in a semi-span configuration. Also, the team found that the upper balance system, which is used for full-span testing, was a straightforward monolithic design. The upper balance system, shown in Figure 6.4-1, is a single-piece construction balance that incorporates flexures and a spline mounting that allows for thermal expansion and contraction in the system.

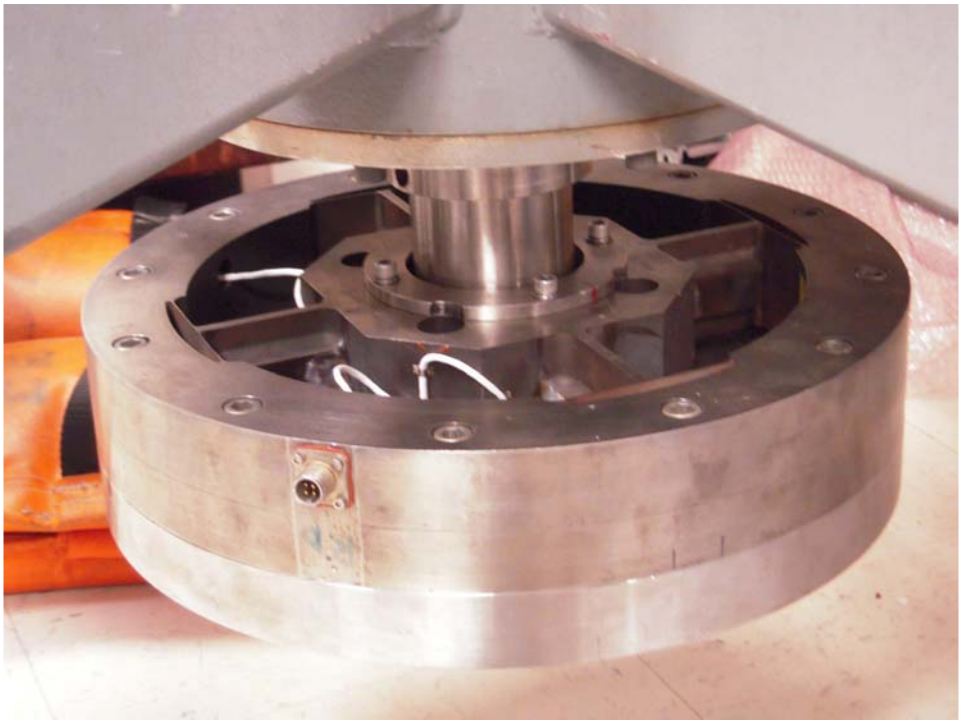

Figure 6.4-1. Upper Balance System

Three upper balance systems with different load ranges currently exist so the load ranges can be set for each test by changing between the various balances. Therefore, the team's focus was applied to generating concepts that would be highly efficient for semi-span testing. These concepts could be used in conjunction with the existing upper balance system when full-span testing was required. The team developed four key concepts that involved complete system upgrades using new turntables and new force measurement balance systems. The main differences in the concepts involved was whether the FMSs were grounded to the wind tunnel or grounded to the basement floor and whether a monolithic or multi-piece constructed FMS was used. Conceptual diagrams of these four systems are shown in Figures 6.4-2 through 6.4-5. Concept key advantages and key disadvantages are discussed separately.

The four concepts that were generated for the lower balance system include combinations of systems that are grounded to the wind tunnel structure or systems that are grounded directly to the floor/earth. The main advantage of grounding the system to the tunnel structure, as shown in Figures 6.4-2 and 6.4-5, is that the balance system moves with the thermal expansion of the tunnel. This reduces the possibility of fouling and changes in the relative position of the model to the test section. This is the method that most aerodynamic tests use when they have sting-mounted model systems. The main disadvantage to grounding the system to the tunnel is that often these types of systems experience more dynamics than systems that are tied to solid ground. The reverse is true when a balance system is grounded to the floor, as shown in Figures 6.4-3 and 6.4-4. Floor-grounded systems tend to have less dynamic inputs; however, thermal movement of the tunnel system relative to the balance can cause fouling and can result in changes in the relative position of the model in the test section.

6.4.1 Concept Number One: Multi-piece Balance Grounded to the Wind Tunnel Structure

The first lower balance system concept, shown in Figure 6.4-2, is an improvement on the existing system concept. It incorporates a multi-piece construction external balance system that is composed of linkages and load cells to measure the forces and moments. The balance system would be grounded to the wind tunnel test section structure.

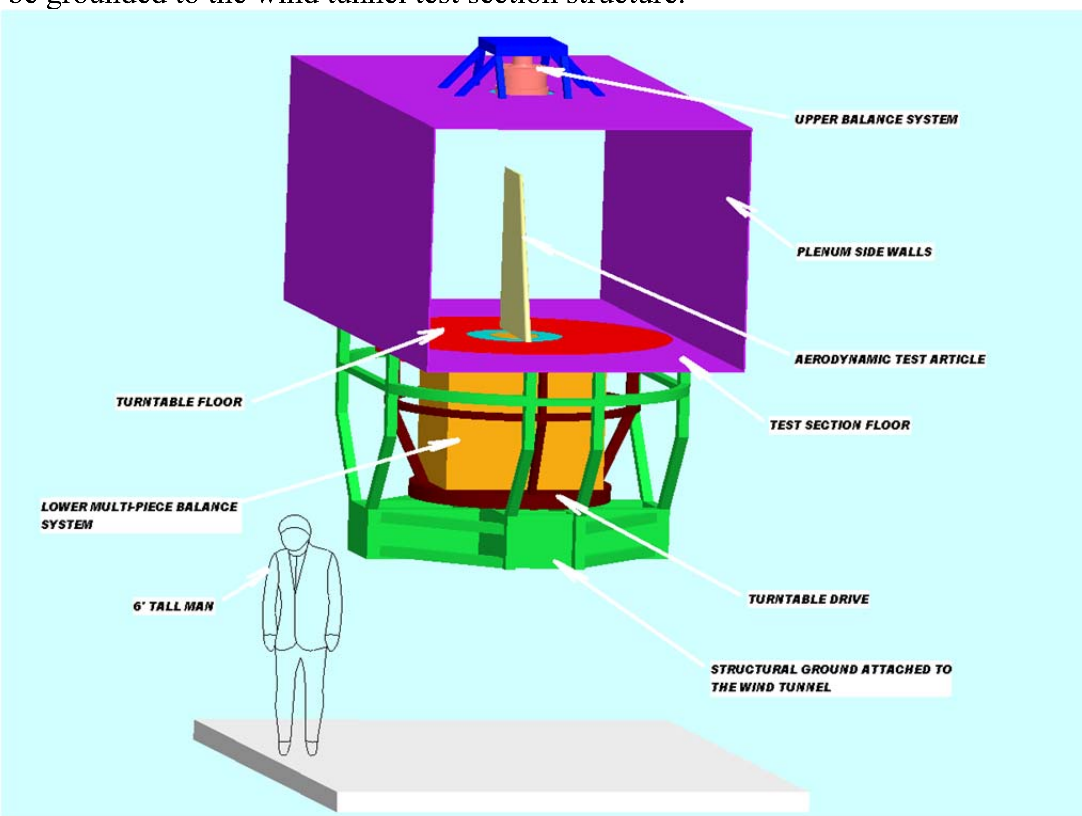

Figure 6.4-2. Multi-piece Balance and Turntable that is Mounted on the Tunnel Structure

Advantages of this system are its relatively low cost and the ability to change load ranges by changing out load cells. While changing out load cells is appealing, the ability to change load cells in a multi-piece balance to adjust the load range is often not practical. Depending on the external balance design, the logistics of changing out load cells while the balance is installed can be challenging. Also, the balance characteristics change so much that a new full calibration is required. Disadvantages include the large physical size, which would hinder model installation and would also make the initial system installation difficult, possibly causing significant tunnel downtime. The initial calibration would be performed at the manufacturing site, but subsequent calibrations would need to be performed in place, requiring tunnel shutdown.

6.4.2 Concept Number Two: Multi-piece Balance Grounded to the Floor

The second concept, shown in Figure 6.4-3, uses the same type of multi-piece balance construction except it would be grounded to the floor instead of grounded to the tunnel.

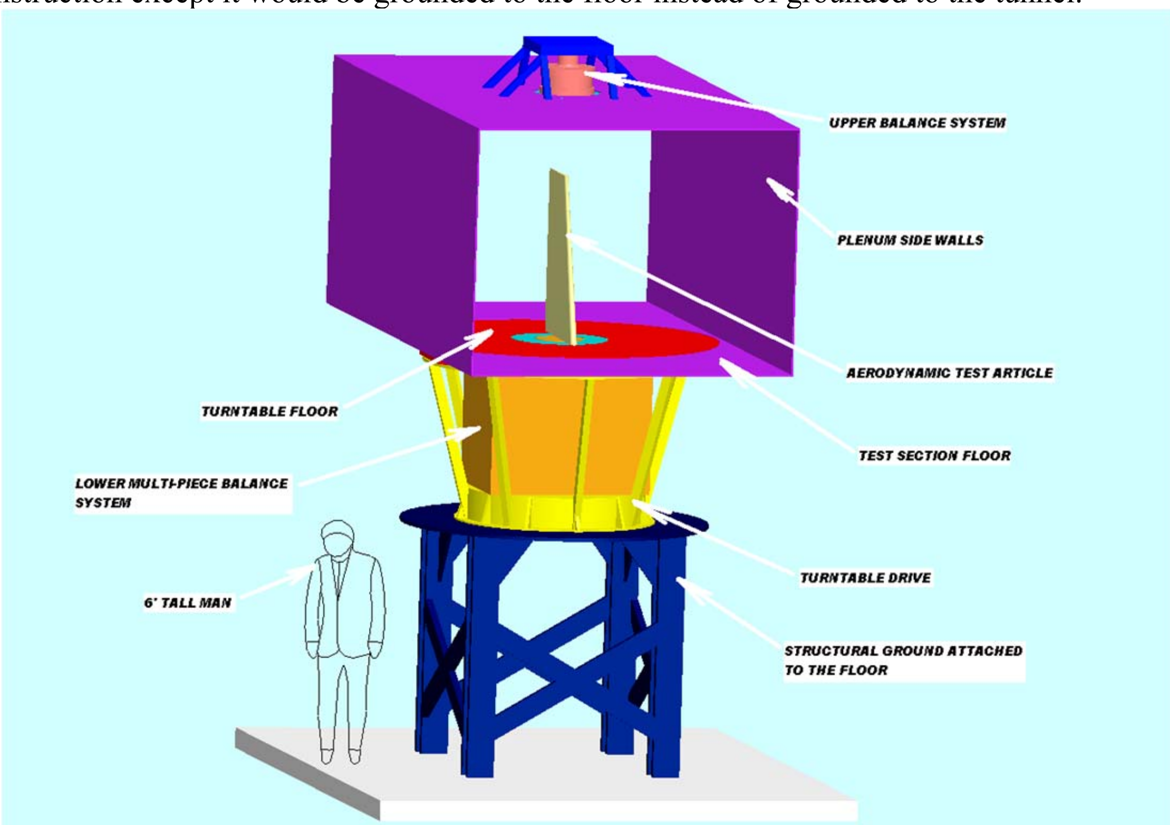

Figure 6.4-3. Multi-piece Balance and Turntable that is Floor-Mounted

Advantages for this system are similar to those of the previous concept; however, this system would be easier to install since it would not have to be adapted to the existing tunnel structure. An added disadvantage would be that the grounding stand would be an added obstacle to the tunnel technicians as they install models in the tunnel. Also, by having the tunnel grounded at a different place than the balance, it is critical that a thorough system analysis be performed to ensure that the tunnel movement due to vibration and thermal affects would not cause issues with the model position relative to the flow. Also, the clearance gaps between the metric balance and the non-metric tunnel floor would have to be analyzed to ensure that acceptable dimensions would be maintained.

6.4.3 Concept Number Three: Monolithic Balance Grounded to the Floor

A third concept, shown in Figure 6.4-4, includes using a monolithic balance and grounding it on a stand through the floor below the tunnel.

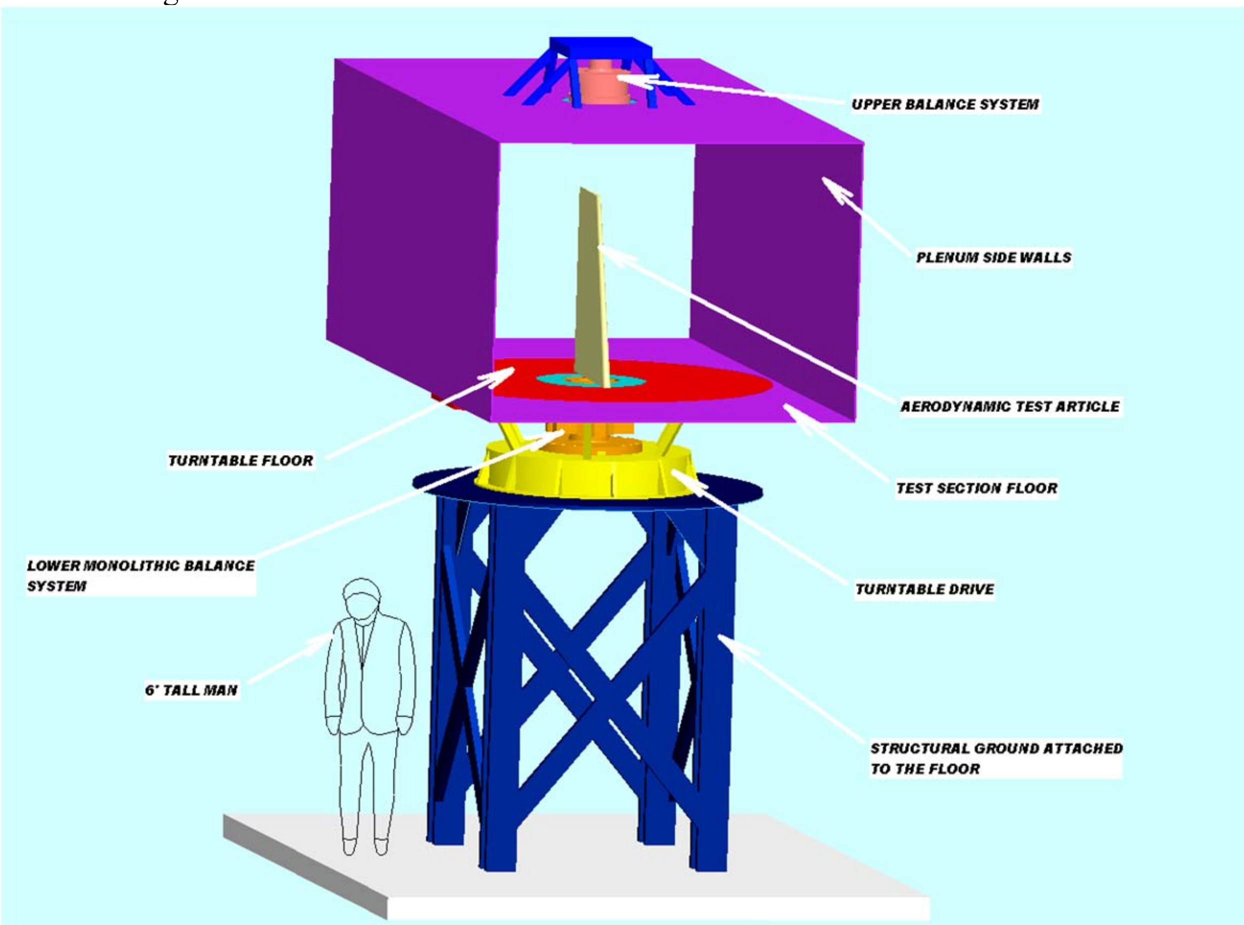

Figure 6.4-4. Monolithic Balance and Turntable that is Floor-Mounted

In this concept, the monolithic balance would typically cost more than the previously mentioned multi-piece balances. However, the single-piece balance would be able to be easily removed for calibration away from the facility. This would allow the facility to replace the live balance with a dummy balance and run tests that do not require force measurements while the balance calibration is being updated at another lab. The disadvantages would be similar to those of the previous concept. The grounding stand would be an obstacle to the technicians installing models in the tunnel.

6.4.4 Concept Number Four: Monolithic Balance Grounded to the Wind Tunnel Structure

The final concept included the use of a monolithic balance that is grounded to the wind tunnel test section and is shown in Figure 6.4-5. This is the concept that the team would recommend if a complete new system was developed; more details of the advantages and disadvantages of this system are discussed.

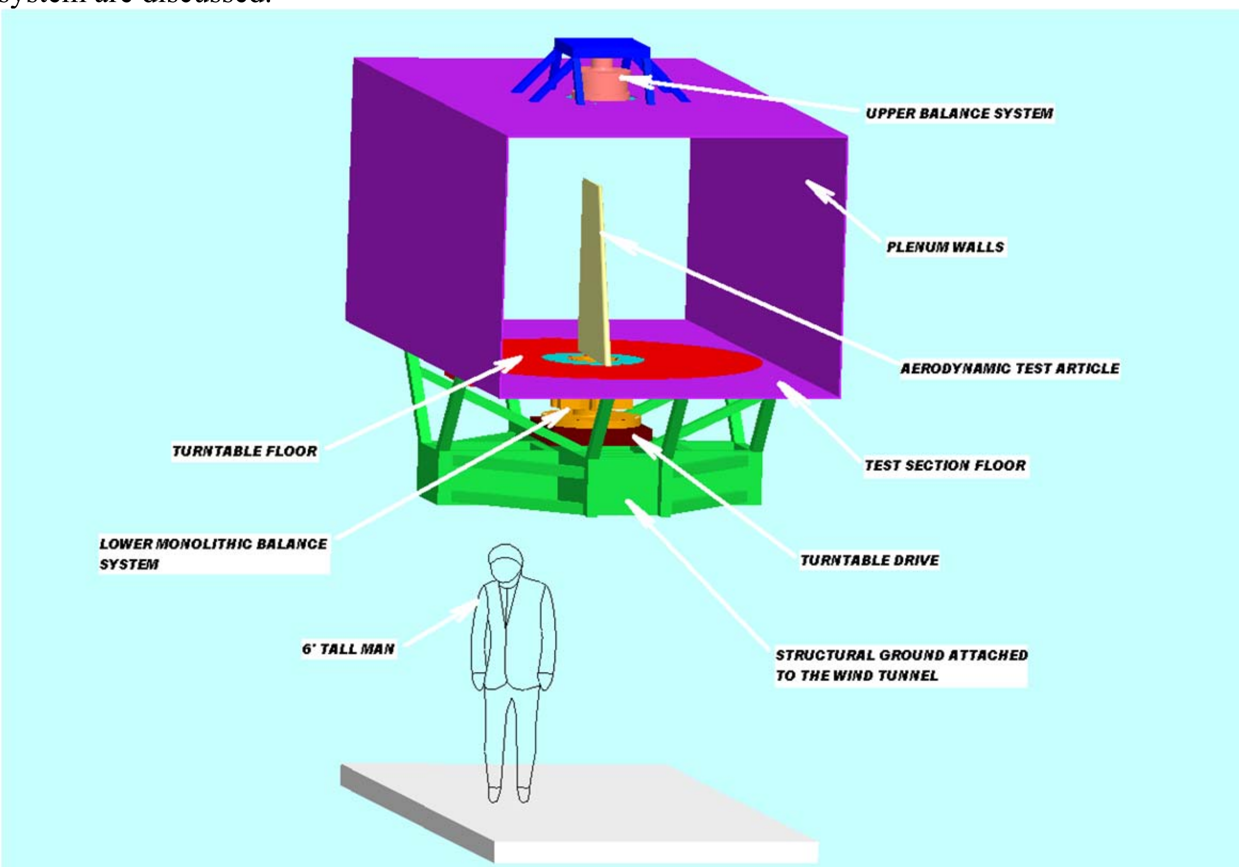

Figure 6.4-5. Monolithic Balance and Turntable that is Mounted on the Tunnel Structure

This concept optimizes the tunnel efficiency for the operators. A significant advantage for this concept is that the single-piece balance is robust and rarely needs to be calibrated and would be able to be easily removed for calibration away from the facility when it does require calibration. Similar to the third concept, this would allow the facility to replace the live balance with a dummy balance and run tests that do not require force measurements while the balance calibration is being updated at another lab. When used for semi-span testing, the manufacturer's calibration coefficients could be used and, with only a few check loads applied, most aerodynamic tests could be performed. This would reduce the facility downtime by eliminating most of the pre-test system calibration effort that is currently required. Also, since this balance is grounded to the tunnel test section, it operates in a similar manner to balances that are internally mounted in models used in typical wind tunnel tests. By having the same ground, the balance moves with the tunnel, and there is less concern with changes in flow alignment with the measuring system and less concern about maintaining the metric and non-metric gaps. Mounting the balance to the tunnel also allows technicians full access under the balance and turntable system, which improves the ability to install models in the test section.

The main disadvantage of the single balance concept is the initial cost of the monolithic balance. These balances are typically expensive since they require complex machining to create multiple measuring elements from a single piece of material. However, when looking through NASA's balance inventory, the team found a blank (i.e., a partially constructed balance) that could possibly be used in this case to defer costs. This balance could then be part of a set of existing semi-span balances that could possibly be borrowed from other NASA facilities to change the load ranges when necessary for a test. One advantage, relative to the IRT for this type of balance, is that for the IRT only two forces and one moment need to be measured. This greatly simplifies the balance design so that a new, custom three-component balance would not be as expensive as a six-component balance of this size. Of course, if balances from other facilities are not available to be borrowed, then a related disadvantage of the monolithic balance approach is that a second monolithic balance would be required for cases where changing the balance is necessary to optimize accuracy. Another consideration for the monolithic balance upgrade approach is that even with a single monolithic balance designed to operate over the entire load range of the IRT, it will likely be able to meet the 1-percent accuracy specification and be more accurate than the current multi-balance FMS.

6.5 Proposed In-Situ Check-Load/Calibration Method

6.5.1 Introduction

This section on a proposed in-situ check-load/calibration method is included within this report to address three of the requests listed in Section 6.2:

- The loads will be measured within +/–1 percent of full scale.
- The force balance system shall have an internal calibration system so no loads are required to be applied inside of the test section.
- It is important to note that initial discussions clearly indicated that the throughput and test efficiency were potentially more important than increasing the accuracy of the FMS. Testing efficiency is critical for meeting the heavy demand for test time in this specialized wind tunnel.

While the request to have an internal calibration system is not included in any of the concepts, the proposed method addresses the accuracy and efficiency requirements. Additionally, a minimum set of check loads is recommended for the FMS for verifications that result in loads needing to be applied in a test section.

6.5.2 Calibration and Verification

Verification and calibration should be based on the requirements of the system. The requirements for the force balance system are listed in Section 6.2. The accuracy requirement is stated as follows: "The loads shall be measured within +/–1 percent of full scale." A review of selected previous calibrations was conducted. The results of a calibration from 2010 are shown in Table 6.5-1.

Table 6.5-1. Force Balance Calibration 2010, Summary Worksheet

	Standard Deviation of Back-Computed Residuals*					
Angle of Attack	**Lift**	**Lift**	**Drag**	**Drag**	**Moment**	**Moment**
Alpha	**Initial Constants**	**Final Constants**	**Initial Constants**	**Final Constants**	**Initial Constants**	**Final Constants**
Degrees	**Std Dev % FS**	**Std Dev % FS**	**Std Dev %FS**	**Std Dev % FS**	**Std Dev % FS**	**Std Dev % FS**
–20.0	0.2	0.1	0.8	0.1	1.3	1.7
–10.0	0.2	0.1	0.7	0.0	1.0	1.0
0.0	0.2	0.1	1.5	0.4	1.3	1.2
10.0	0.2	0.1	0.7	0.1	1.3	1.1
20.0	0.2	0.1	0.7	0.1	1.4	1.1
All	**0.2**	**0.1**	**0.9**	**0.1**	**1.3**	**1.2**

*Standard Deviation of Back-Computed Residuals: The standard deviation of the computed residuals from the loads applied during the calibration. These calibration loads were also used to develop the calibration matrix.

The initial constants columns are the residuals computed using the original load-cell-only calibrations, while the final constants are the residuals computed using the in-situ calibration. While there is improvement in the residuals for drag using the final constants, lift and pitch are essentially the same. Also, the requirement of +/–1 percent is satisfied for lift and drag using the initial constants and slightly missed for pitch. Observing that the initial constants nearly meet the accuracy requirement leads to the following proposed calibration (i.e., verification) methodology:

- Apply check loads to verify the initial calibration constants.
- Develop check-load/calibration hardware to reduce the check-load/calibration/ verification time to less than one shift (if possible).
- If the verification is not satisfactory (i.e., does not meet the 1-percent requirement), then apply additional loads, if necessary, to compute a new set of calibration constants that account for in-situ effects, such as interactions.

The proposed approach will apply for all four scenarios listed below:

1) Existing balance in semi-span mode.
2) Existing balances in full-span mode**.
3) New balance in semi-span mode.
4) New balances in full-span mode**.
   ** See Section 6.5.3 for full-span check-loads/calibration discussion.

As noted in Section 6.5.3, the full-span model is an exception. When both the lower and upper balance systems are used, there is a higher probability of requiring a full in-situ calibration due to the model-dependent stiffness effects.

6.5.3 Calibration Load Schedule and Hardware Design

Based on the proposed approach and the objectives of the assessment, the most efficient method to develop the load schedule is to use design of experiments (DOE) [ref. 4]. DOE is a statistically based approach to maximize the amount of information obtained for a given amount of resources and provide objective/quantifiable knowledge. Additionally, to take full advantage of DOE and the requirement to reduce the loading to one shift, new calibration hardware is proposed that enables the most efficient execution of the load schedule.

A principle of DOE is to make each data point as information rich as possible. Therefore, applying this to force measurement calibration equates to applying as many load components as is practical per load point. Table 6.5-2 presents the proposed load schedule utilizing a factorial design approach while taking into account the hardware capabilities (the load magnitudes are based on the 2010 calibration referenced previously). The calibration design can be scaled as needed to adjust for different full-scale load requirements. A subset of this load schedule can be utilized for check loads initially. If the computed residuals (i.e., the difference between the computed and applied loads) are within the required accuracy, then the verification is complete. However, if the residuals are not acceptable, then the remainder of the schedule can be executed to develop a new in-situ matrix.

Table 6.5-2. DOE Calibration Load Schedule

Actuator Load Position	Full Load Points	Lift	Drag	Pitch	Applied Load	Load Angle	Pitch Distance
		(lbs)	(lbs)	(ft-lbs)	(lbs)	(degrees)	(inches)
1	1	–3000	1000	2000	3162	–18.4	–8
10	2	3000	0	2000	3000	0.0	8
3	3	–3000	1000	–2000	3162	–18.4	8
6	4	3000	1000	–2000	3162	18.4	–8
8	5	3000	1000	2000	3162	18.4	8
zero	6	0	0	0	0		
5	7	–3000	0	–2000	3000	0.0	8
zero	8	0	0	0	0		
7	9	3000	0	–2000	3000	0.0	–8
zero	10	0	0	0	0		
2	11	–3000	0	2000	3000	0.0	–8
Mid Point Loads (same positions as above, and can be easily applied after setup)							
1	12	–1500	500	1000	1581	–18.4	–8
10	13	1500	0	1000	1500	0.0	8
3	14	–1500	500	–1000	1581	–18.4	8
6	15	1500	500	–1000	1581	18.4	–8
8	16	1500	500	1000	1581	18.4	8
5	17	–1500	0	–1000	1500	0.0	8
7	18	1500	0	–1000	1500	0.0	–8
2	19	–1500	0	1000	1500	0.0	–8

Note: actuator load positions 4 and 9 apply only a lift force. This is not required for the calibration but is easy to apply and provides additional information if needed for assessment or troubleshooting.

The load schedule will enable computation of the coefficients for the following model:

$$R_i = a_i + \sum_{j=1}^{n} b_{i,j}\, F_j + \sum_{j=1}^{n}\sum_{k=1}^{n} F_j\, F_k$$

where $i = 1\ to\ 3$ and $j \neq k$.

This is more than required for verifying the existing system calibration, but it enables interactions to be included if needed.

The calibration hardware required to execute the loadings is shown in Figure 6.5-1.
Figure 6.5-2 shows all of the planned actuator positions; however, ***only one actuator is required per loading.*** The positions are shown for tension loadings only. Typically, tension loads are more easily aligned. However, if compression loads are possible with the hardware and can be

shown to maintain accuracy, utilizing compression loads will further cut the number of configurations in half.

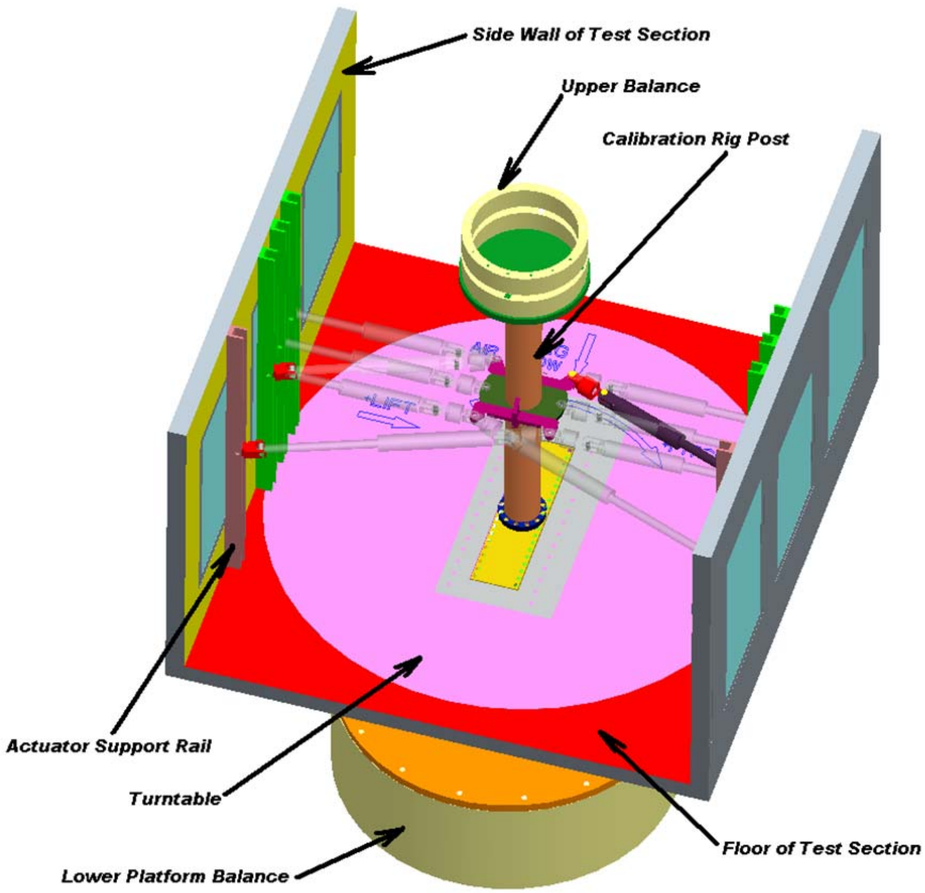

Figure 6.5-1. Check-Load/Calibration Hardware Required to Execute the Loading

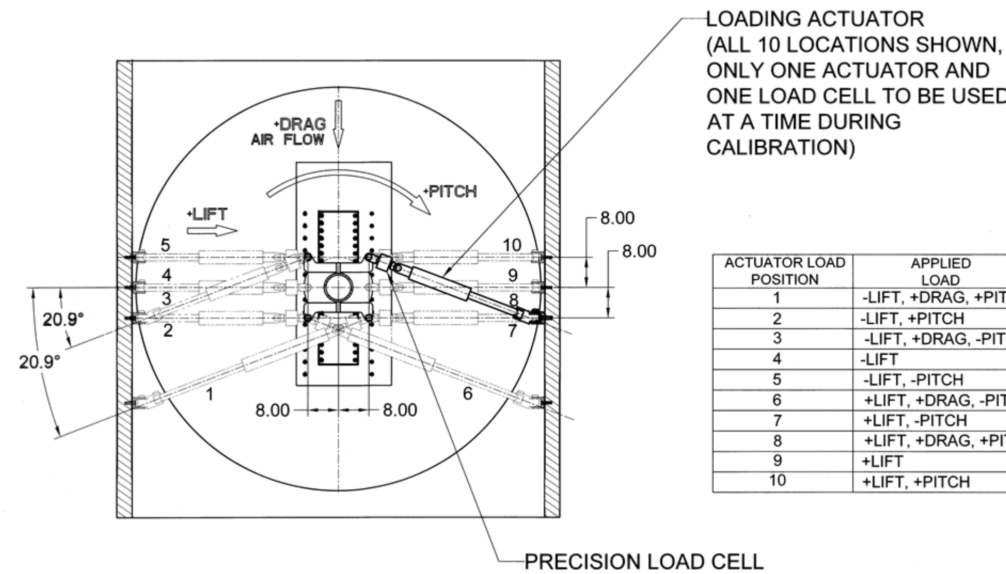

ACTUATOR LOAD POSITION	APPLIED LOAD
1	-LIFT, +DRAG, +PITCH
2	-LIFT, +PITCH
3	-LIFT, +DRAG, -PITCH
4	-LIFT
5	-LIFT, -PITCH
6	+LIFT, +DRAG, -PITCH
7	+LIFT, -PITCH
8	+LIFT, +DRAG, +PITCH
9	+LIFT
10	+LIFT, +PITCH

Figure 6.5-2. Actuator Positions Required for Check-Load/Calibration Loadings

The hardware consists of attach points to the tunnel wall in the form of rails bolted in place with pre-determined actuator pin locations. The system uses the same actuator and load cells that are currently used for applying loads augmented with additional length rods as needed. A new piece of hardware with actuator attach points is needed to provide the necessary locations on the center post.

6.5.4 Full-Span Configuration: Check-Loads/Calibration

The full-span configuration presents a unique scenario for the FMS. The uniqueness is due to the influence of the test article on the measurement performance. When the upper and lower balance systems are connected through the test article, the amount of load each will measure is dependent on the stiffness of the test article. Therefore, it is recommended that each full-span test article have a full set of loads applied to develop an in-situ calibration matrix. It is understood that it will be difficult to apply loads to the test articles in certain configurations and the check-load approach can be used. This is a typical approach that is used when a full calibration is not feasible; however, accuracies of less than 0.25 percent are typically the goal in this situation.

An assessment of the test article stiffness impact on the calibration can be executed using dummy test articles with different spring constants as calibration hardware. Performing a minimum of two calibrations to bound varying model system stiffness can provide a quantitative assessment of the impact by comparing the calibration residuals and the coefficient differences.

7.0 Data Analysis

7.1 Current System Information

Literature detailing the structural design, calibration rationale, and total system accuracies is almost nonexistent, so the team held multiple technical interchanges with the facility personnel to gather as much data as possible. An initial list of requirements was supplied by the facility personnel and is listed in Section 6.2. It is extremely important to reiterate that initial discussions with facility personnel clearly indicated that the throughput and test efficiency was potentially more important than just increasing the accuracy of the FMS. Testing efficiency was a critical aspect of meeting the heavy demand for test time in this specialized wind tunnel. Since this throughput and test efficiency was not directly listed in the requirements, the NESC team developed the following list of evaluation metrics shown in Table 7.1-1.

Table 7.1-1. System Evaluation Metrics

Order of Importance	Evaluation Metrics
1	Productivity (test throughput, ease of use/calibration, training for new system)
2	Reliability
3	Facility Impacts (downtime, facility modification)
4	Capability (higher loads, AOA)
5	Cost
6	Accuracy Improvement (AOA, loads)

These metrics were used to judge the various FMS concepts and select the most appropriate system for recommendation to the IRT.

7.2 Turntable Measurement Data

During the initial site visit, observations of the turntable operation and visual inspections of the mechanisms led to the belief that that the turntable setting angle, and thus the model AOA, would be a significant source of error in the delivered aerodynamic coefficients. The existing turntable motion mechanism is an old system that uses multiple bolt shanks as gear teeth for the ring gear. The control system has been updated to slowly move to command positions. This helps reduce positioning error in the gear system. The slow positioning is an area where throughput can be improved with a newer turntable system with a faster rotational speed. A plan was developed to quantify the angle setting accuracy of the turntable; the measurements were completed on a subsequent site visit.

To measure the absolute angle of rotation of the turntable, a Theodolite[1] was placed on the center of rotation of the turntable. The center mark was scribed in the floor plates of the turntable. An alignment laser was mounted off the turntable and aligned with the center mark; the turntable

[1]http://en.wikipedia.org/wiki/Theodolite (Accessed on September 24, 2012)

was rotated through its range of motion and the center mark stayed within the laser dot, confirming the center location. Also, spirit levels were placed on the turntable as it was rotated through its range of motion. The turntable rotation plane was level within +/–20 seconds (based on one division of the spirit levels).

The Theodolite was placed such that its rotation axis was coincident with the turntable axis, and the Theodolite was leveled. There are optic components in the Theodolite that assist with this position adjustment. A target, comprised of finely printed vertical lines, was taped to the downstream turning vanes. The target was approximately 111 feet from the Theodolite; see Figure 7.2-1 and Figure 7.2-2.

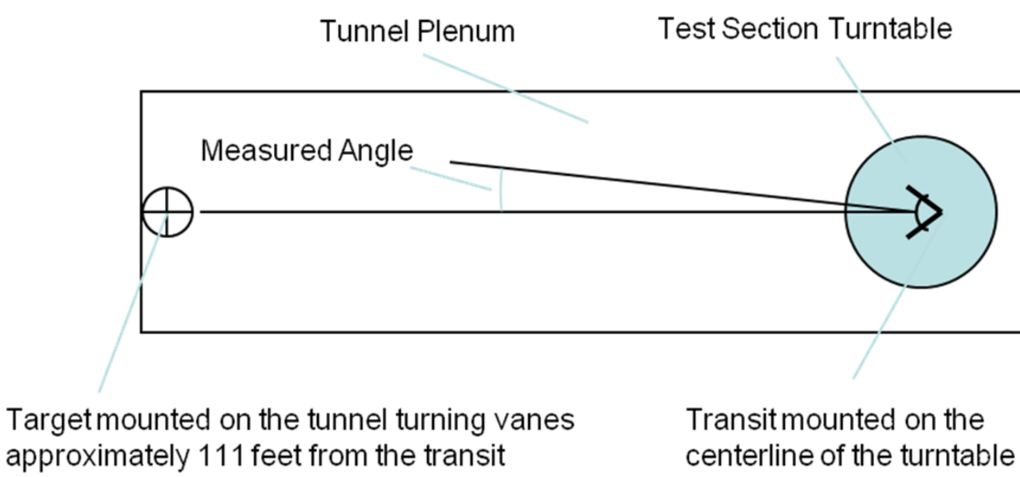

Figure 7.2-1. Overhead Sketch of the Turntable Angle Measurement System

Turntable measurement setup. Theodolite is placed at the center of the turntable. The target can be seen taped to the down stream turning vanes. The target was comprised of fine vertical lines.

Figure 7.2-2. Photograph of the Turntable Measurement Setup

The turntable was commanded to the start position. The Theodolite was set on the target, and the readout was zeroed. The turntable was then commanded to a new position. Once the motion stopped, the Theodolite was used to reacquire the target, and the absolute angle was read and recorded. This was repeated through several yaw runs.

The turntable was rotated in a unidirectional manner from positive to negative; see Table C-1, Appendix C. The turntable was then rotated in a unidirectional manner from negative to positive, as shown in Table C-2, Appendix C. This should be the best-case measurements as the slop or backlash in the drive system is removed. Also, a random run was performed such that the slop or backlash of the drive system was not minimized; see Table C-3, Appendix C.

Several observations were noted while acquiring the data. There was a 0.08- to 0.10-degree offset between the set point angle and the feedback angle. This could probably be resolved with a setting in the control software. The average error for all runs was –0.08 degrees, and the standard deviation in the error for all runs was approximately 0.03 degrees. The angle errors are highest at the highest angles, as shown in Figure 7.2-3.

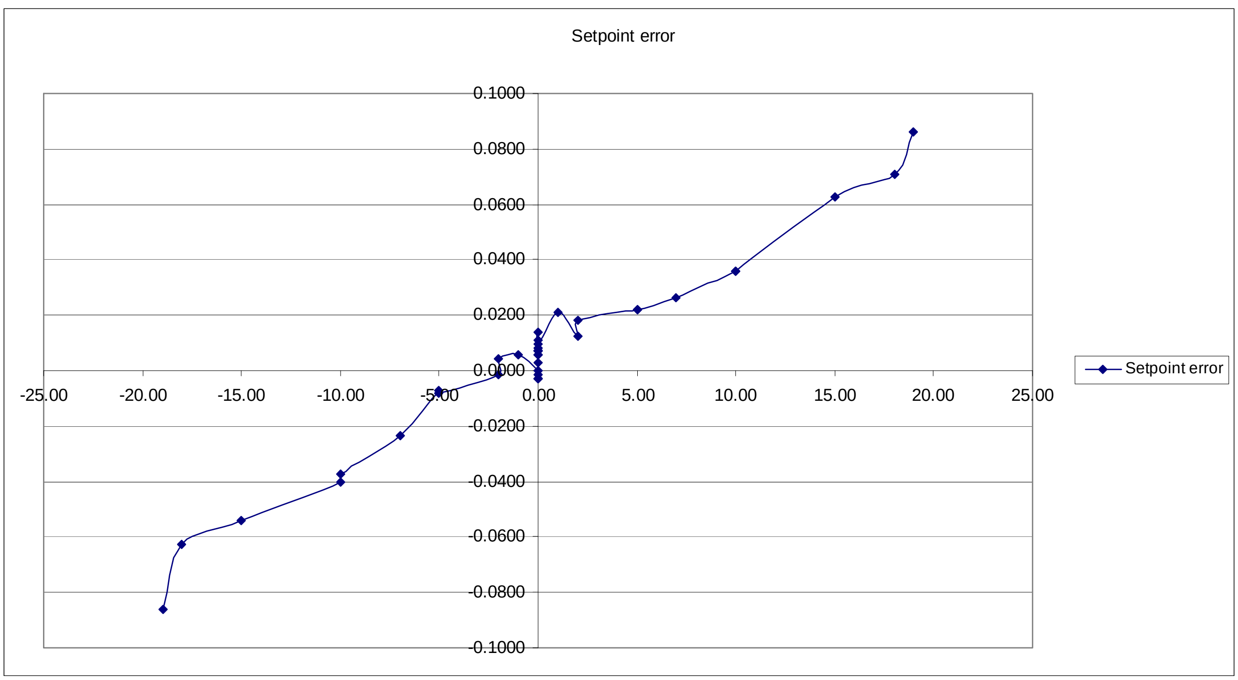

Figure 7.2-3. Set Point Error versus Turntable Angle

The average of the error when zero was commanded was 0.005 degrees. The turntable angle accuracy appears to be much better than initially anticipated and was not a significant contributor to the uncertainty in the aerodynamic coefficient calculations, at least when tested at ambient room temperature conditions without a temperature gradient or cold test section.

7.3 Uncertainty Analysis

The total error estimate in a measurement is the combination of systematic (β) and random (ε) errors. Systematic error is that portion of the total error that remains constant in repeated measurements throughout the test. Random error is that portion of the total error that varies randomly in repeated measurements throughout the test and adds "scatter" to the data. The relationship between the two error sources is depicted in Figure 7.3-1. The random error component is seen as a distribution centered about the mean of the measurement. The systematic error is an offset of this mean from the true (unknown) value. In this analysis, the random error distribution is assumed to be approximately normal (Gaussian).

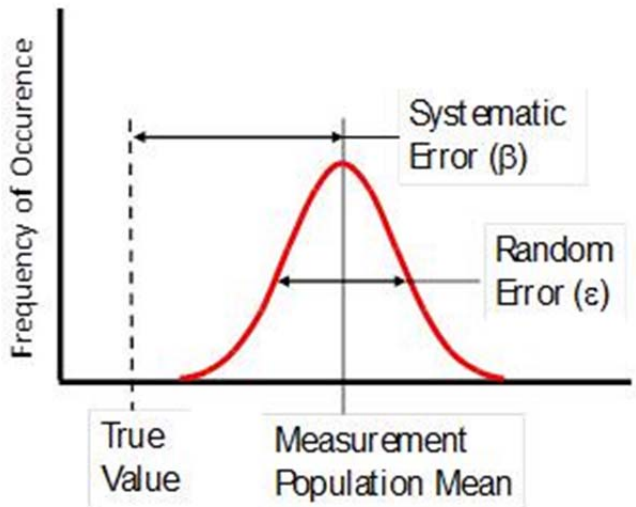

Figure 7.3-1. Relationship between Two Error Sources

The uncertainty analysis of the existing and proposed new external lower balance system was based on a representative semi-span wing test case. To calculate system uncertainties, force and moment estimates were chosen based on historical data from a semi-span wing model geometry with ice shapes consistent with IRT testing. The model has a chosen wing area (S) of 5.8 square feet, semi-span ($b/2$) of 4.5 feet, and AOA (α) of 12 degrees. The lift coefficient (C_L) is approximately unity with a drag coefficient (C_D) of approximately 0.14. The chosen operating dynamic pressure (q) is approximately 100 psf. Load cell component loads were calculated using the representative aerodynamic forces and moments, balance geometry, and load cell configuration.

7.3.1 Analysis of the Existing IRT Lower Balance System

A simplified uncertainty analysis was performed for the existing external lower balance system. The uncertainty in force and moment coefficients was estimated. This estimate is later compared with a similar set of estimates for the recommended concept number four. This comparison allows the IRT personnel to generate an understanding of the impact an upgrade will have on their future aerodynamic test data.

7.3.1.1 Overview and Assumptions

Full-span model force measurement testing in the IRT requires the simultaneous use of an upper and lower balance system. Using both of these balance systems for full-span model testing will generate unique uncertainties for specific models. These uncertainties must be developed for each full-span model. It was decided that using only the floor balance in the uncertainty analysis would generate enough information to gain confidence in system upgrade decisions. Therefore, the existing upper balance system was not included in this analysis. The following assumptions were used to perform the uncertainty analysis for the external lower balance system.

- Force and moment coefficients were functions of the independent variables AOA (α), dynamic pressure (q), and the three primary load cells (R_A, R_B, and R_C) only.
- Sources of uncertainty associated with the data acquisition and signal conditioning system were assumed to be small compared with the aforementioned sources and negated.
- Thermal effects were not considered in this analysis and may be significant.
- The Taylor-Series Method (TSM) of combining multiple sources of systematic error with the assumption of negligible correlations is adequate for comparison purposes [refs. 1 and 3].
- Elemental systematic error source contributions are estimated by manufacturer's specifications and/or available calibrations.
- A 95-percent confidence level was chosen in keeping with engineering practice and as recommended in the references.
- A single semi-span test case was chosen as representative for this analysis.
- Actual wind tunnel test data were not made available. Since random error estimates are best computed with repeated measurements using the entire FMS (end to end), they are not included in this analysis but could be accounted for later if/when data become available. The method for inclusion of random uncertainty contributions to overall uncertainty is provided.

7.3.1.2 Layout of IRT Lower Balance System

The lower external balance metric frame is supported vertically by three flexures. Force on the frame is reacted in the axial direction through the axial load cell R_A. Load cells R_B and R_C are located 1.25 feet west (x_B) and east (x_C) of the balance center and measure normal force (N) and pitching moment (PM). The schematic diagram shown in Figure 7.3-2 shows the location of the load cells and links with respect to the metric frame. A dashed outline shows the location of a semi-span wing model. The metric frame rotates with the turntable through the AOA.

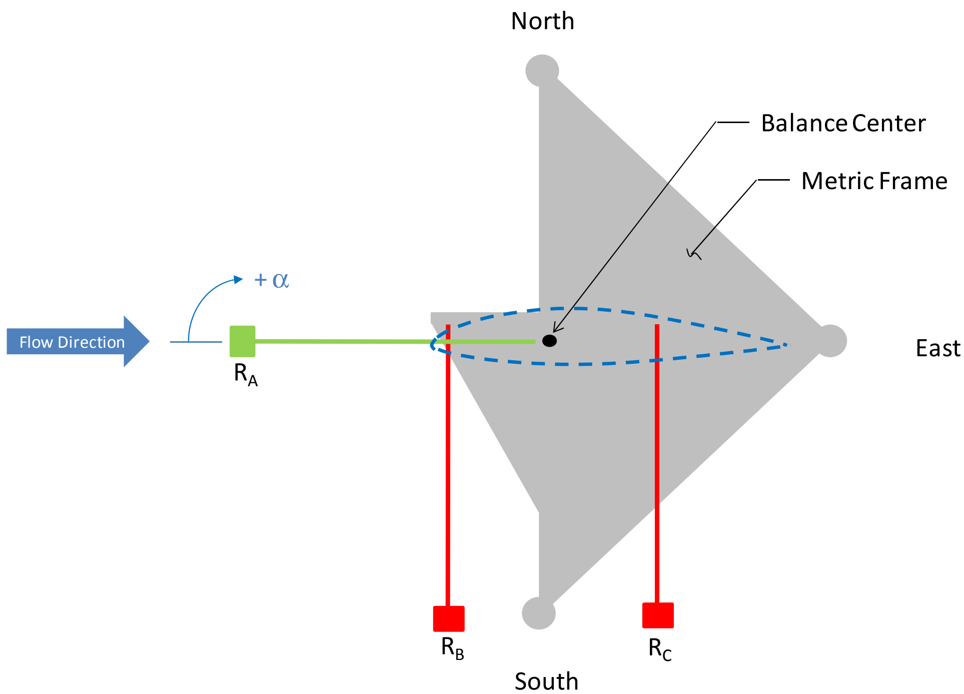

Figure 7.3-2. Current IRT-FMS Schematic Diagram

7.3.1.3 Data Reduction Equations

Force component resolution is shown in the vector diagram in Figure 7.3-3. Forces and moments from load cells are calculated assuming that tension in the load cell link causes a positive force.

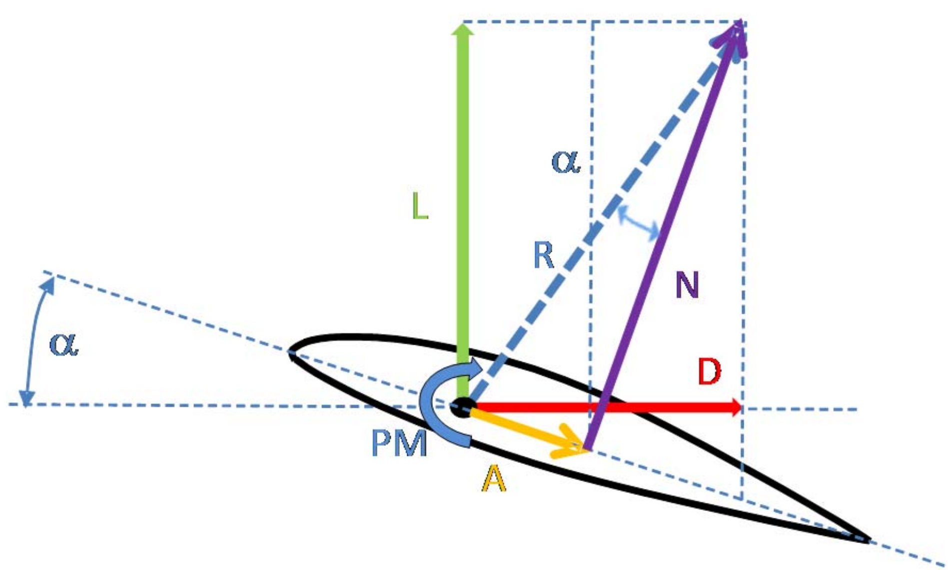

Figure 7.3-3. Forces and Moments on the Model and Aerodynamic Coefficients

The resulting data reduction equations (DREs) are summarized below. The normal (*N*) and axial (*A*) forces are combined in resultant (*R*). *R* is resolved into component forces lift (*L*) and drag (*D*).

$$N = R_B + R_C$$
$$A = R_A$$
$$L = N\cos(\alpha) - A\sin(\alpha) = (R_B + R_C)\cos(\alpha) - R_A\sin(\alpha)$$
$$D = N\sin(\alpha) + A\cos(\alpha) = (R_B + R_C)\sin(\alpha) + R_A\cos(\alpha)$$
$$PM = R_B x_B - R_C x_C$$

The C_D, C_L, and pitching moment coefficient (C_m) are calculated. *S* is the wing area; *q*, the dynamic pressure; and *c*, the chord length.

$$C_D = \frac{D}{qS} = \frac{(R_B + R_C)\sin(\alpha) + R_A\cos(\alpha)}{qS}$$
$$C_L = \frac{L}{qS} = \frac{(R_B + R_C)\cos(\alpha) - R_A\sin(\alpha)}{qS}$$
$$C_m = \frac{PM}{qSc} = \frac{R_B x_B - R_C x_C}{qSc}$$

7.3.1.4 TSM Uncertainty Analysis

Consider a general case where an experimental result *r* is a function of *j* measured variables X_j, called the DRE.

$$r = r(X_1, X_2, X_3, \ldots, X_j)$$

If the measured variables X_j may be assumed independent, then the overall uncertainty U_r in the result *r* may be expressed as:

$$U_r^2 = b_r^2 + s_r^2$$

where the overall uncertainty is partitioned into systematic uncertainty contributions (b_r) and random uncertainty contributions (s_r). When they are defined at the standard deviation level, they are called the standard values and are combined using a root sum square as shown above. The systematic standard uncertainty contribution may now be written as the sum of contributions from the elemental sources.

$$b_r^2 = \sum_{i=1}^{j}\left(\frac{\partial r}{\partial X_i}\right)^2 b_{X_i}^2$$

The overall systematic standard uncertainty may be found best through estimating the individual elemental source contributions (b) using calibration results and manufacturer's specifications and combining them. Using the TSM and the DRE for the existing balance, the systematic standard uncertainty in a given force coefficient (C_F) may be found as:

$$b_{C_F} = \left[\left(\frac{\partial C_F}{\partial R_A} b_{R_A} \right)^2 + \left(\frac{\partial C_F}{\partial R_B} b_{R_B} \right)^2 + \left(\frac{\partial C_F}{\partial R_C} b_{R_C} \right)^2 + \left(\frac{\partial C_F}{\partial \alpha} b_\alpha \right)^2 + \left(\frac{\partial C_F}{\partial q} b_q \right)^2 \right]^{\frac{1}{2}}$$

All elemental source contributions b_{X_i} are stated at the standard deviation level.

The random error contribution to the overall measurement is best estimated experimentally. For instance, replicate C_D measurements will allow calculation of a standard deviation.

The general methodology outlined here is applicable to all of the measured forces and moments. Individual source values and partial derivative terms are tabulated in Appendix A. The uncertainty calculations for C_D are given below as a sample.

Starting with the DRE for C_D:

$$C_D = \frac{D}{qS} = \frac{(R_B + R_C)\sin(\alpha) + R_A \cos(\alpha)}{qS}$$

Partial derivative terms are calculated next:

$$\frac{\partial C_D}{\partial R_A} = \frac{\cos\alpha}{qS}$$

$$\frac{\partial C_D}{\partial R_B} = \frac{\partial C_D}{\partial R_C} = \frac{\sin\alpha}{qS}$$

$$\frac{\partial C_D}{\partial \alpha} = \frac{R_C \cos\alpha + R_B \cos\alpha - R_A \sin\alpha}{qS}$$

$$\frac{\partial C_D}{\partial q} = -\frac{R_C \sin\alpha + R_B \sin\alpha + R_A \cos\alpha}{q^2 S}$$

The total systematic standard uncertainty in C_D may be found as:

$$b_{C_D} = \left[\left(\frac{\partial C_D}{\partial R_A} b_{R_A} \right)^2 + \left(\frac{\partial C_D}{\partial R_B} b_{R_B} \right)^2 + \left(\frac{\partial C_D}{\partial R_C} b_{R_C} \right)^2 + \left(\frac{\partial C_D}{\partial \alpha} b_\alpha \right)^2 + \left(\frac{\partial C_D}{\partial q} b_q \right)^2 \right]^{\frac{1}{2}}$$

The random and systematic uncertainty estimates are combined for an estimate of the total standard uncertainty. At this time, sufficient data were not available for random uncertainty estimates. At such a time that data are available, the random and systematic standard uncertainty contributions may be combined as shown below.

$$u_{C_D}^2 = b_{C_D}^2 + s_{C_D}^2$$

A confidence interval about the sample mean value of C_D is formed using the expanded uncertainty U. Expanded uncertainty values are found using the product of a coverage factor and the total standard uncertainty (which by definition is at the standard deviation level). The recommended coverage factor is the student's t statistic for the appropriate degrees of freedom (DOF).

$$U = t \cdot u_{C_D}$$

Using a 95-percent confidence interval and assuming that the large sample assumption is satisfied (DOF > 30), the coverage factor may be assumed as 2. For adjustment of the coverage factor for small samples, see reference 1.

$$U_{95} = 2 \cdot u_{\bar{x}}$$

Individual C_D results may now be reported with a confidence interval using the mean value bounded by the confidence interval +/–U. Using the method described here under the assumptions outlined allows the user to report a bound on a mean drag coefficient ($\overline{C}_D$). This is the interval within which the true result resides with the chosen confidence of 95 percent.

$$C_D = \overline{C}_D \pm U_{95}$$

7.3.1.5 Overall IRT Existing Lower Balance System Uncertainty Results

The systematic uncertainty expressed as an expanded value (e.g., $2b_{C_D}$) for each of the measured coefficients is tabulated in Table 7.3-1. Detailed calculations for all tables can be found in Appendix A. The percent of nominal value expresses the expanded systematic uncertainty as a percent of the nominal coefficient at the given representative conditions.

Table 7.3-1. Coefficients and Estimated Uncertainty of the Current FMS

	C_D	C_L	C_m
Expanded Systematic Uncertainty	0.005	0.024	0.024
Nominal Coefficient Value	0.147	1.02	–0.083
% of Nominal	3.54	2.32	28.3

Using the available system information, an analysis revealed a system uncertainty value for the C_m to be 28 percent. While there were no clear uncertainty requirements for system acceptability, it is evident that a 28-percent error is not desired. However, indications from the available system calibration led the team to believe that an updated set of data could reduce this uncertainty.

7.3.1.6 Possible Improvements for the IRT Existing Lower Balance System Uncertainty Results

Using the available data, an uncertainty analysis revealed the major sources of error in the existing IRT balance as the component normal force load cell calibration accuracies. The performance of the existing balance could be improved by choosing load cells with improved accuracy. Commercially available load cells of the same capacity can offer 0.05 percent of full-scale accuracy and better versus the 0.2 percent currently in use. If the higher accuracy normal force load cells (0.05 percent) were used with the same semi-span test case of this analysis, the following uncertainties would result (see Table 7.3-2). To further consider component contributions to overall uncertainty, see Appendix A, where details are presented.

Table 7.3-2. Coefficients and Estimated Uncertainty of the Current FMS with Updated Load Cells

	C_D	C_L	C_m
Expanded Systematic Uncertainty	0.002	0.006	0.006
Nominal Coefficient Value	0.147	1.02	–0.083
% of Nominal	1.22	0.582	7.07

7.3.2 Analysis of the Proposed New IRT Lower Balance

A simplified uncertainty analysis was performed for the recommended FMS, concept number four, and is described in Section 6.4.4. The uncertainty in the force and moment coefficients was estimated. This estimate is later compared with the previously generated set of estimates for the existing IRT lower balance system. This comparison allows the IRT personnel to generate an understanding of the impact an upgrade will have on their future aerodynamic test data.

7.3.2.1 Overview and Assumptions

The uncertainty in the force and moment coefficients was estimated under the following assumptions.

- Force and moment coefficients were functions of the independent variables AOA (α) and dynamic pressure (q) and the measured components normal (N), axial (A), and pitching moment (PM) only.
- Sources of uncertainty associated with the data acquisition and signal conditioning system were assumed to be small compared with the aforementioned sources and negated.
- Thermal effects were not considered in this analysis.

- The TSM of combining multiple sources of systematic error with the assumption of negligible correlations is adequate for comparison purposes.
- Elemental systematic error source contributions are estimated by manufacturer's specifications and/or available calibrations of similar existing balance designs.
- A 95-percent confidence level was chosen in keeping with engineering practice and as recommended in the references.
- A single semi-span test case was chosen as representative for this analysis.

7.3.2.2 Layout of Proposed Semi-span Style Monolithic Lower Balance System in IRT

The monolithic lower balance system is mounted such that it rotates with the turntable through the AOA. The schematic diagram in Figure 7.3-4 shows the location of the balance as a shaded circle. A dashed outline shows the location of a semi-span wing model.

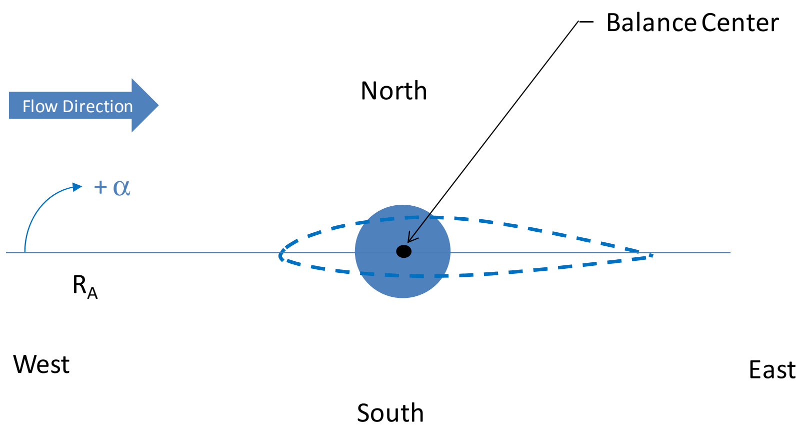

Figure 7.3-4. Proposed Lower Monolithic Balance Layout

7.3.2.3 Data Reduction Equations

Force component resolution is shown in the vector diagram in Figure 7.3-5. The proposed monolithic balance design measures the normal (N), axial (A), and pitching moment (PM) components directly (i.e., forces/moments are not resolved through multiple load cells).

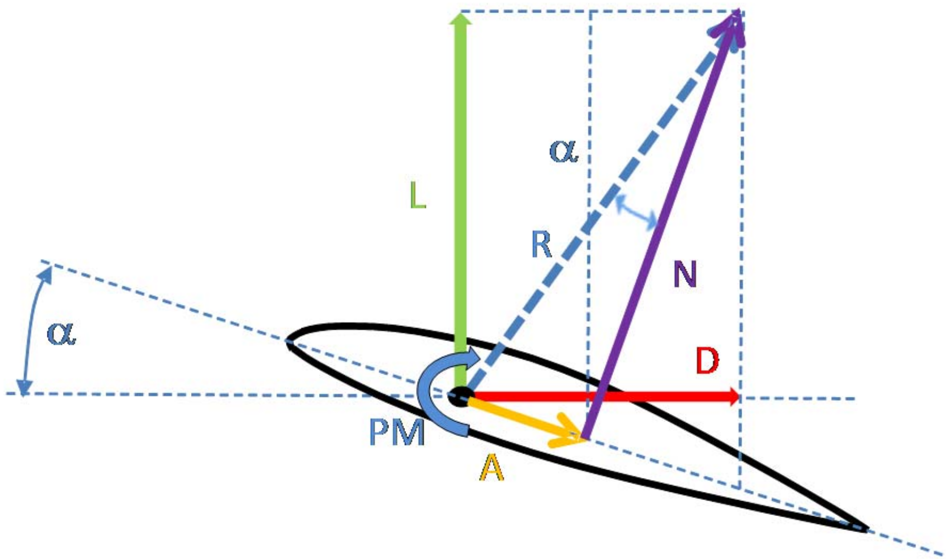

Figure 7.3-5. Forces and Moments on the Model and Aerodynamic Coefficients

The resulting DREs are summarized below. The normal (*N*) and axial (*A*) forces are combined in resultant (R). R is resolved into component forces lift (*L*) and drag (*D*).

$$L = N\cos(\alpha) - A\sin(\alpha)$$
$$D = N\sin(\alpha) + A\cos(\alpha)$$

C_D, C_L, and C_m are calculated in terms of balance force components. *S* is the wing area; *q,* the dynamic pressure; and *c,* the chord length.

$$C_D = \frac{D}{qS} = \frac{N\sin(\alpha) + A\cos(\alpha)}{qS}$$
$$C_L = \frac{L}{qS} = \frac{N\cos(\alpha) - A\sin(\alpha)}{qS}$$
$$C_m = \frac{PM}{qSc}$$

7.3.2.4 TSM Uncertainty Analysis

The TSM approach is identical to that discussed in Section 7.3.1.4. Using the TSM and the DRE for the new balance, the systematic standard uncertainty in the C_D may be found as:

$$b_{C_D} = \left[\left(\frac{\partial C_D}{\partial N} b_N \right)^2 + \left(\frac{\partial C_D}{\partial A} b_A \right)^2 + \left(\frac{\partial C_D}{\partial \alpha} b_\alpha \right)^2 + \left(\frac{\partial C_D}{\partial q} b_q \right)^2 \right]^{\frac{1}{2}}$$

The general methodology is applicable to all of the measured forces and moments. Individual source uncertainty values and partial derivative terms are tabulated in Appendix A. The uncertainty calculations for the C_D are given below as a sample.

Starting with the DRE for C_D:

$$C_D = \frac{D}{qS} = \frac{N\sin(\alpha) + A\cos(\alpha)}{qS}$$

Partial derivative terms are calculated next.

$$\frac{\partial C_D}{\partial N} = \frac{\sin\alpha}{qS}$$

$$\frac{\partial C_D}{\partial A} = \frac{\cos\alpha}{qS}$$

$$\frac{\partial C_D}{\partial \alpha} = \frac{N\cos\alpha - A\sin\alpha}{qS}$$

$$\frac{\partial C_D}{\partial q} = -\frac{N\sin\alpha + A\cos\alpha}{q^2 S}$$

The systematic standard uncertainty in C_D may be found as:

$$b_{C_D} = \left[\left(\frac{\partial C_D}{\partial N} b_N \right)^2 + \left(\frac{\partial C_D}{\partial A} b_A \right)^2 + \left(\frac{\partial C_D}{\partial \alpha} b_\alpha \right)^2 + \left(\frac{\partial C_D}{\partial q} b_q \right)^2 \right]^{\frac{1}{2}}$$

The random and systematic uncertainty estimates are combined for an estimate of the total standard uncertainty. At this time, sufficient data were not available for random uncertainty estimates. At such a time that data are available, the random and systematic standard uncertainty contributions may be combined as:

$$u_{C_D}^2 = b_{C_D}^2 + s_{C_D}^2$$

A confidence interval about the sample mean value of C_D is formed using the expanded uncertainty *U*. Expanded uncertainty values are found using the product of a coverage factor and the total standard uncertainty (which by definition is at the standard deviation level). The recommended coverage factor is the student's *t* statistic for the appropriate DOF.

$$U = t \cdot u_{C_D}$$

Using a 95-percent confidence interval and assuming the large sample assumption is satisfied (DOF > 30), the coverage factor may be assumed as 2. For adjustment of the coverage factor for small samples, see reference 1.

$$U_{95} = 2 \cdot u_{\bar{x}}$$

Individual C_D results may now be reported with a confidence interval using the mean value bounded by the confidence interval +/–*U*. Using the method described here under the assumptions outlined allows the user to report a bound on a mean drag coefficient ($\overline{C}_D$). This is the 95-percent confidence interval where the true result resides.

$$C_D = \overline{C}_D \pm U_{95}$$

7.3.2.5 Overall Proposed New IRT Floor Balance Uncertainty Results

The systematic uncertainty expressed as an expanded value (e.g., $2b_{C_D}$) for each of the measured coefficients is tabulated in Table 7.3-3. The percent of nominal value expresses the expanded systematic uncertainty as a percent of the nominal coefficient at the given representative conditions.

Table 7.3-3. Coefficients and Estimated Uncertainties of Proposed Single Piece Lower Balance FMS

	C_D	C_L	C_m
Expanded Systematic Uncertainty	0.002	0.005	0.005
Nominal Coefficient Value	0.147	1.02	–0.083
% of Nominal	1.45	0.495	6.00

7.3.3 Conclusions

In conclusion, the estimated uncertainties of various recommended FMS upgrades can be compared in Table 7.3-4. From the comparison chart, it can be seen that the greatest overall uncertainty improvement will be generated by the team's primary recommendation to replace the lower balance system with a new monolithic balance. By updating the normal force load cells, large uncertainty improvements can be made; however, this will not generate any throughput efficiencies that will be incurred using a monolithic balance system.

Table 7.3-4. Estimated Uncertainties of Proposed FMS

	C_D	C_L	C_m
Current FMS Estimated Uncertainty % of Nominal	3.54	2.32	28.3
Updated FMS with Updated NF Load Cells % of Nominal	1.22	0.5817	7.07
Updated FMS with Single-Piece Balance % of Nominal (Similar accuracies are expected for concepts 1 through 4)	1.45	0.495	6.00

Upgrading the FMS with a single-piece balance and a new turntable system will yield uncertainty estimates similar to upgrading with a single-piece balance. The main advantage of upgrading the turntable would be a more efficient test setup and increased test throughput efficiency.

It should be noted that no data were provided for the measurement of dynamic pressure and the analysis uses an estimated value based on typical pressure transducer accuracies. The current axial load cell of the existing balance has an uncertainty value, which is expressed as a percentage of reading compared with the proposed balance, which is stated as a percentage of full scale. Therefore, the uncertainty in C_D for higher drag test articles will increase for the existing balance as a percentage of nominal aerodynamic coefficient but decrease for the proposed new monolithic balance. While a thermal analysis was not possible, the monolithic design is expected to be more robust to thermal effects than a multi-piece balance design.

7.4 Structural Review

As part of the design trade and configuration evaluation, the existing structure was investigated to determine whether the load path of a new turntable or load balance should be tied to the tunnel structure or taken directly to ground. The team also assessed the breadth of structural modifications that would be required to accommodate the recommended design changes. Note that a structural stress analysis was not conducted as part of this assessment. The observations and recommendations in this section are only based on visual inspections of the existing structure, review of the drawings and existing analyses, and interviews with those familiar with the IRT operations.

7.4.1 Summary

Recommendation 2, installing a new monolithic balance and a new turntable system, will yield the highest productivity and the most reliable approach. Structural analyses and modifications would be recommended to remove all unnecessary redundant structures and to start with the cleanest/simplest interface for a new modern model support system/turntable. The existing structure appears to be adequate so the modifications would primarily be cleaning up/simplifying and verifying the new load paths to ground. If Recommendation 3 is pursued, namely to install a modern monolithic balance on the top of the existing turntable, the upgrade would utilize the existing load path. Therefore, the upgrade should be adequate for the full established capacity of the wind tunnel unless it is limited by the capacity of the particular monolithic balance that is installed. Since there are no known problems with the existing structure, it would appear that the upgrade could be performed without structural modifications, except where necessary, to properly provide a mounting interface for the monolithic balance on top of the turntable cruciform. Also, since it utilizes the existing load path, a full stress analysis to ground would not be required. Recommendation 4 involves replacing the load cells within the existing balance system with more accurate loads cells. Load cell replacement does not involve a structural modification; therefore, no structural calculations or analysis should be required for this option.

7.4.2 Background/Observations

Primarily from inspecting the existing structural loads paths, it can be seen that there have been several past modifications to the load path and structure since the tunnel was originally constructed. In the original structural arrangement, metric loads were beamed through the tunnel structure and down through the floor of the area beneath the test section into an actual balance room, as shown in Figure 7.4-1.

Figure 7.4-1. Load Path Termination in Tunnel. The photo shows the former cylindrical balance columns now mounted to blocks of concrete. This is directly beneath the floor area that is below the test section/turntable/balance system.

There appears to be evidence of several generations of modifications and changes since that time, including the complete removal of the balance room. However, the original vertical load paths are still present with the flexures at the top; these appear to be anchored to the floor area. It appears that with most of these layered updates and modifications, previous structural load paths and fixtures were not removed unless necessary, so the current structure appears to be redundant and, as a result, indeterminate. As stated above, because no issues with this existing load path are evident, a minimal cost upgrade could be implemented using this same philosophy without modifying the existing load path. However, it is recommended that the stress analyses be reviewed and perhaps a new stress analysis be initiated, including a finite element model (FEM) of the complete load path to ground. Due to the redundancy of the structural load path, it may also be desirable to add strain gauges to the existing structure in key locations to validate the results of the FEM. If an upgrade to the turntable is desired, then a full structural analysis/FEM would also be required since a new turntable would not be designed to attach to the current indeterminate, redundant load paths.

The Recommendation 3 option to upgrade the existing system by installing a monolithic balance onto the existing turntable could require modification to both the turntable plate and supporting cruciform. In all, the modifications required appear to be relatively minor and should not diminish the load capability or significantly alter the existing load path of the system. Select support beams welded to the underside of the turntable plate could require removal to accommodate overhead installation of the monolithic balance. The tube spanning the distance from the cruciform to the turntable plate would also need to be removed. Further modification of the cruciform would also be needed to provide a sufficient mounting surface for the balance. The portion of the supporting cruciform and its interface to the tube can be seen in Figure 7.4-2.

Figure 7.4-2. Turntable Cruciform Base and Support Tube

Installing the monolithic balance on top of the existing turntable cruciform would eliminate the labor- and time-intensive need to install the existing FMS balance assembly. This would significantly increase the accessibility to the interior of the test models; however, the IRT operations staff indicated the desire to remove more of the existing structure for even better access to the interiors of models mounted in the test section. Based only on the visual inspection of the existing structure and the highly redundant loads paths, this does not appear possible without a full structural analysis. A complete FEM could be exercised to completely identity many of the old structural remnants from past configurations that could be removed. This would most likely include the three vertical posts that originally transferred the loads to the long removed balance room, but still tie to the floor beneath the test section. The resulting structure/design could be optimized for maximum access to the test section or for other operational needs. A detailed FEM would also be required to pursue the Recommendation 2 option to mount a new monolithic balance on a new turntable. For this upgrade option, most if not all of the hardware/structure for the existing turntable and FMS would be removed, and the new system would be optimized for maximum model access and reliability.

8.0 Findings, Observations, and NESC Recommendations

8.1 Findings

The following findings were identified:

F-1. For the IRT, throughput/efficiency is equally or more important than force measurement accuracy. The focus on throughput and efficiency greatly increases the importance of certain aspects, such as model access during buildup, calibration setup and performance, installation and removal of the lower balance system, etc.

F-2. As stated in Appendix B, the current calibration loads are not applied near the model center of pressure. Loading at the center of pressure generates calibration data that are similar to what will be experienced in wind tunnel testing. For best practices, one would "calibrate as you test."

F-3. Calibration loads for full-span and semi-span models are applied to a fixture that is removed and replaced by a model for wind tunnel testing, and no on-model check-loads are typically applied.

F-4. Upper balance systems (multiple ranges) that are used for full-span model testing have monolithic construction and were designed to allow thermal expansion and contraction.

F-5. The current calibration procedure has been inherited over the years, and the logic of why loads are applied as listed in the current load schedule has been lost.

F-6. The largest source of uncertainty in measured aerodynamic force and moment coefficients when using the current FMS was found to be the normal force load cells stated calibration accuracies.

F-7. The uncertainty analysis of the existing FMS for a typical semi-span wing test article reveals the following uncertainty values of the computed aerodynamic coefficients:

C_D: 3.5 percent

C_L: 2.3 percent

C_m: 28 percent

F-8. The existing turntable positioning accuracy is +/–0.03 degrees, measured at room temperature with no model loads. This accuracy is more than adequate to meet the facility needs of 0.05 degrees. However, no measurements or estimates were made to determine how this accuracy may change with loads, cold temperatures, or temperature gradients that likely exist during operation.

F-9. Based on interviews with the tunnel operations crew, the existing turntable and FMS structure makes it difficult to build up complex models with multiple pass-through lines.

8.2 Observations

The following observations were identified:

O-1. The current FMS and turntable system contain a conglomeration of many generations of updates and modifications that have been implemented over the life of this facility, including partial removals, abandoned-in-place structures, and mechanisms from the previous updates and modifications. Although the current system is working and appears to have adequate positioning accuracy for the turntable, if a problem were to occur within this old system, it may be difficult to diagnose or repair, especially since those familiar with the last modification/update (about 20 years ago) have since retired.

O-2. The existing turntable motion mechanism is an old system that actually uses multiple bolt shanks as the gear teeth for the ring gear and, although it appears to provide the desired accuracy, when measured at uniform ambient room temperature, it is most likely not as robust as more modern turntable mechanisms would be.

O-3. Testing productivity would likely be increased with a faster rotating turntable that could reposition the model to the desired AOA more quickly.

8.3 NESC Recommendations

The following NESC recommendations are directed toward the IRT and Aeronautics Research Mission Directorate (ARMD) and are listed in the order of assessed priority. Recommendation 1 is the minimum suggested action the IRT and ARMD should implement. Recommendation 1 will improve both the throughput and the productivity during the calibration/check-load procedures for the current FMS and for any of the following FMS recommendations that may be implemented. Recommendation 2 results in the highest productivity, the highest accuracy, and the most reliable FMS, but it has the highest estimated cost. Recommendations 3 and 4 offer improvement, reliability, and lower estimated costs. However, the efficiency and test throughput will be less than for Recommendation 2. Table 8.3-1 is a comparison of the recommendations and includes cost estimates and benefit statements. It should be noted that the cost estimates include only design, manufacturing, and installation costs; no other criteria were incorporated into the estimates.

R-1. Modify the calibration hardware to enable the ability to apply loads about wind tunnel model centers of pressure, which would require changing the check load/calibration procedures used at the facility, entail developing and documenting a new calibration schedule, and potentially involve developing new calibration spreadsheet software.

Modifying calibration procedures for the current FMS would include:

a) Apply check-loads about the center of pressure of the wind tunnel model to ensure that the uncertainty of the FMS meets the test requirements. If the check-load uncertainties in this step meet the test requirements, then steps b, c, and d are not required.

b) For semi-span testing, perform an in-situ calibration applying loads about the center of pressure.

c) Perform in-situ model calibrations when testing a full-span model.

d) Document any new calibration methodology, including the logic of why loads are applied in specific circumstances. ***(F-2, F-3, F-4, F-5)***

R-2. Incorporate a new model support and turntable system with a new monolithic balance with continued use of the existing upper balance systems for full-span testing to attain the maximum desired results of force measurement accuracy and throughput. ***(F-1, F-4, F-5 F-6, F-7, F-9, O-1, O-2)***

R-3. If R-2 is not implemented, then develop a new monolithic balance mounted on the existing turntable with continued use of the existing upper balance systems for testing full-span models to improve in the calibration throughput, increase system force measurement accuracies, and improve productivity. ***(F-1, F-4, F-5 F-6, F-7, F-8, F-9)***

R-4. If neither R-2 or R-3 are implemented, then replace the normal force load cells with higher accuracy (0.05 percent or better full-scale) models with continued use of the existing upper balance systems for full-span testing. This improvement represents the most cost-effective method to reduce the uncertainty of the aerodynamic coefficients to C_D, 1.22 percent; C_L, 0.582 percent; and C_m, 7.07 percent. ***(F-6, F-7, F-8)***

Table 8.3-1. Cost Range Estimates for FMS Upgrade Recommendations

Recommendation #	Design Cost Range ($)	Manufacturing and Installation Cost Range ($)	Benefit
R-1	40K to 50K	60K to 170K	Significant increase in calibration knowledge at low cost (calibrate as you test), and significant increase of end-to-end system confidence in uncertainties.
R-2	185K to 200K	640K to 735K	Significant increase in accuracy and most significant increase in throughput. The system can be designed with a focus on minimizing model change effort.
R-3	105K to 135K	300K to 400K	Significant improvement in accuracy and throughput with medium expenditure.
R-4	10K to 15K	25K to 40K	Significant increase in accuracy with low cost (no throughput benefits)

Two examples of how to interpret/combine the cost estimates follow:

1. If the IRT were to implement R-1, the total cost estimates would be generated by adding the Design Cost Range with the Manufacturing and Installation Range to get a total estimated cost range of $100K to $220K (low cost equals $40K + $60K; high cost equals $50K + $170K).
2. If the IRT were to implement R-1 and R-2, the total cost would be generated by adding the total cost ranges of R-1 with those of R-2. R-2 would have a total estimated cost range of $825K to $935K (low cost equals $185K + $640K; high cost equals $200K + $735K). Therefore, the total estimated cost range to implement both R-1 and R-3 would be $925K to $1,155K (low cost equals $100K (from example 1 above) + $825K; high cost equals $220K (from example 1 above) + $935K).

A similar methodology would be used to calculate the estimated cost ranges for a combination of R-1 and R-3 or for a combination of R-1 and R-4.

9.0 Alternate Viewpoints

There were no alternate viewpoints identified within the NESC team or the NRB quorum during the course of this assessment.

10.0 Other Deliverables

There are no other deliverables for this assessment.

11.0 Lessons to Learn

LL-1. A thorough analysis of perceived component uncertainties is always prudent. While the group consensus centered on poor turntable positioning performance, actual surveys showed otherwise (supported by F-8).

LL-2. When operating and calibrating a test and measurement system such as this IRT and the associated force balance system, it is important to include an expert in the type of systems being used either on a regular basis as part of the operations team or, as a minimum, to occasionally review and optimize the related procedures. In this case, the experts on the NESC assessment team have presented Recommendation 1, which highlights several improvements in the calibration process that both simplify the process and improve the overall calibration accuracy. These include both applying the calibration loads to as near the center of pressure as possible and recognizing that the full-span model support load/force distribution is dependent on the model stiffness and, therefore, should be calibrated on the actual model or something that simulates the model stiffness instead of the rigid calibration beam that is currently used.

LL-3. When incorporating a model pass-through (e.g., air lines, wiring, pressure measurement lines), it is best to incorporate long “soft” lines paralleling the balance system. This way, the balance system carries the majority of the loads as it is designed to do.

LL-4. It is good practice to apply the maximum loads on the model that are expected in a wind tunnel test to get a high confidence of the system uncertainties and to check any pass-through for unacceptable fouling. Note that this is often overlooked during test preparation.

LL-5. It is wise to find instrumentation experts to act either as advisors or as smart buyers for program and facility major instrumentation purchases and upgrades. Purchasing instrumentation systems without expert advice can be costly to NASA and can result in delivery of a less-than-optimal system or one that does not actually meet program needs.

12.0 Recommendations for NASA Standards and Specifications

No recommendations for NASA standards and specifications were identified as a result of this assessment.

13.0 Definition of Terms

Corrective Actions	Changes to design processes, work instructions, workmanship practices, training, inspections, tests, procedures, specifications, drawings, tools, equipment, facilities, resources, or material that result in preventing, minimizing, or limiting the potential for recurrence of a problem.
Finding	A conclusion based on facts established by the investigating authority.
Lessons Learned	Knowledge or understanding gained by experience. The experience may be positive, as in a successful test or mission, or negative, as in a mishap or failure. A lesson must be significant in that it has real or assumed impact on operations; valid in that it is factually and technically correct; and applicable in that it identifies a specific design, process, or decision that reduces or limits the potential for failures and mishaps, or reinforces a positive result.
Observation	A factor, event, or circumstance identified during the assessment that did not contribute to the problem, but if left uncorrected has the potential to cause a mishap, injury, or increase the severity should a mishap occur. Alternatively, an observation could be a positive acknowledgement of a Center/Program/Project/Organization's operational structure, tools, and/or support provided.
Problem	The subject of the independent technical assessment.
Proximate Cause	The event(s) that occurred, including any condition(s) that existed immediately before the undesired outcome, directly resulted in its occurrence and, if eliminated or modified, would have prevented the undesired outcome.
Recommendation	An action identified by the NESC to correct a root cause or deficiency identified during the investigation. The recommendations may be used by the responsible Center/Program/Project/Organization in the preparation of a corrective action plan.
Root Cause	One of multiple factors (events, conditions, or organizational factors) that contributed to or created the proximate cause and subsequent undesired outcome and, if eliminated or modified, would have prevented the undesired outcome. Typically, multiple root causes contribute to an undesired outcome.

14.0 Acronyms List

A	Axial
AIAA	American Institute of Aeronautics and Astronautics
AOA	Angle of Attack

C_D	Drag Coefficient
C_F	Force Coefficient
C_L	Lift Coefficient
C_m	Pitching Moment Coefficient
D	Drag
DOE	Design of Experiment
DOF	Degree of Freedom
DRE	Data Reduction Equation
FEM	Finite Element Model
FMS	Force Measurement System
GRC	Glenn Research Center
GSFC	Goddard Space Flight Center
IRT	Icing Research Tunnel
JSC	Johnson Space Center
KSC	Kennedy Space Center
L	Lift
LaRC	Langley Research Center
MSFC	Marshall Space Flight Center
MTSO	Management Technical Support Office
N	Normal
NESC	NASA Engineering and Safety Center
NRB	NESC Review Board
PM	Pitching Moment
q	Dynamic Pressure
R	Resultant
TIM	Technical Interface Meeting
TSM	Taylor-Series Method

15.0 References

1. Coleman H. W. and Steele, G. W.; *Experimentation, Validation, and Uncertainty Analysis for Engineers*, 3rd ed., 2009.
2. "Assessment of Wind Tunnel Data Uncertainty," AIAA S-071A, 1999.
3. "Test Uncertainty," ASME PTC 19.1-2005.
4. Montgomery, D. C.; *Design and Analysis of Experiments*, Eighth Edition, 2012.

16.0 Appendices

Appendix A. Simplified Uncertainty Analysis Calculations
Appendix B. Calibration and Operation of the Force Balance System in the NASA-Glenn 6-ft by 9-ft Icing Research Tunnel
Appendix C. Turntable Measurement Data

Appendix A. Simplified Uncertainty Analysis Calculations

A.1 Existing IRT Lower Balance System

Uncertainty in C_L, starting with the DREs for C_L:

$$C_L = \frac{L}{qS} = \frac{(R_B + R_C)\cos(\alpha) - R_A \sin(\alpha)}{qS}$$

Partial derivative terms are calculated:

$$\frac{\partial C_L}{\partial R_A} = \frac{-\sin\alpha}{qS}$$

$$\frac{\partial C_L}{\partial R_B} = \frac{\partial C_L}{\partial R_C} = \frac{\cos\alpha}{qS}$$

$$\frac{\partial C_L}{\partial \alpha} = \frac{-(R_B + R_C)\sin\alpha - R_A \cos\alpha}{qS}$$

$$\frac{\partial C_L}{\partial q} = \frac{-(R_B + R_C)\cos(\alpha) + R_A \sin(\alpha)}{q^2 S}$$

The absolute standard systematic uncertainty in C_L may be found as:

$$b_{C_L} = \left[\left(\frac{\partial C_L}{\partial R_A} b_{R_A} \right)^2 + \left(\frac{\partial C_L}{\partial R_B} b_{R_B} \right)^2 + \left(\frac{\partial C_L}{\partial R_C} b_{R_C} \right)^2 + \left(\frac{\partial C_L}{\partial \alpha} b_{\alpha} \right)^2 + \left(\frac{\partial C_L}{\partial q} b_{q} \right)^2 \right]^{\frac{1}{2}}$$

Uncertainty in C_m, starting with the DREs for C_m:

$$C_m = \frac{PM}{qSc} = \frac{R_B x_B - R_C x_C}{qSc}$$

Partial derivative terms:

$$\frac{\partial C_m}{\partial R_B} = \frac{x_B}{qSc}$$

$$\frac{\partial C_m}{\partial R_c} = \frac{-x_C}{qSc}$$

$$\frac{\partial C_m}{\partial q} = \frac{-R_B x_B + R_C x_C}{q^2 Sc}$$

The systematic standard uncertainty in C_m may be found as:

$$b_{C_m} = \left[\left(\frac{\partial C_m}{\partial R_B} b_{R_B} \right)^2 + \left(\frac{\partial C_m}{\partial R_C} b_{R_C} \right)^2 + \left(\frac{\partial C_m}{\partial q} b_q \right)^2 \right]^{\frac{1}{2}}$$

Table A-1. Systematic Standard Uncertainty Estimates (*b*) for Existing Balance using Representative Semi-span Icing Model

Description	Symbol	Nominal	Units	*b* (1 Std Dev)	Comments
Load cell for axial	R_A	–40	lbs	–0.08	Stated at 0.4% of reading by calibration supplied by IRT.
Load cell for normal	R_B	275	lbs	5	Stated at 0.2% of FS = 5000 by calibration supplied by IRT.
Load cell for normal	R_C	325	lbs	5	Stated at 0.2% of FS = 5000 by calibration supplied by IRT.
AOA	α	12	deg	0.035	From turntable survey performed in this study.
Dynamic pressure	q	100.8	psf	0.0101	No uncertainty given, chosen as representative.
Wing planform area	S	5.8	ft^2	const	
Arm B	x_B	1.25	ft	const	
Arm C	x_C	1.25	ft	const	
Chord	c	1.29	ft	const	

Drag			Lift			Pitching Moment		
Partial Derivative (PD)		(b*PD)^2	Partial Derivative (PD)		(b*PD)^2	Partial Derivative (PD)		(b*PD)^2
dCD/dRA =	0.0016731	1.79148E-08	dCL/dRA =	-0.0003556	8.09395E-10	-	-	-
dCD/dRB =	0.0003556	3.1617E-06	dCL/dRB =	0.0016731	6.99796E-05	dCm/dRB =	0.0016588	6.87942E-05
dCD/dRC =	0.0003556	3.1617E-06	dCL/dRC =	0.0016731	6.99796E-05	dCm/dRC =	-0.0016588	6.87942E-05
dCD/dalpha =	1.0180710	3.86765E-07	dCL/dalpha =	-0.1464510	8.00342E-09	-	-	-
dCD/dq =	-0.0014529	2.14479E-10	dCL/dq =	-0.0100999	1.03647E-08	dCm/dq =	0.0008228	6.87942E-11

A.2 Proposed New Semi-span IRT Floor Balance

Uncertainty in C_L, starting with the DREs for C_L:

Partial derivative terms:

$$\frac{\partial C_L}{\partial N} = \frac{\cos\alpha}{qS}$$
$$\frac{\partial C_L}{\partial A} = \frac{-\sin\alpha}{qS}$$
$$\frac{\partial C_L}{\partial \alpha} = \frac{-N\sin\alpha - A\cos\alpha}{qS}$$
$$\frac{\partial C_L}{\partial q} = \frac{-N\cos(\alpha) + A\sin(\alpha)}{q^2 S}$$

The systematic standard uncertainty in C_L may be found as:

$$b_{C_L} = \left[\left(\frac{\partial C_L}{\partial N} b_N\right)^2 + \left(\frac{\partial C_L}{\partial A} b_A\right)^2 + \left(\frac{\partial C_L}{\partial \alpha} b_\alpha\right)^2 + \left(\frac{\partial C_L}{\partial q} b_q\right)^2\right]^{\frac{1}{2}}$$

Uncertainty in C_m, starting with the DREs for C_m:

$$C_m = \frac{PM}{qSc}$$

Partial derivative terms:

$$\frac{\partial C_m}{\partial PM} = \frac{1}{qSc}$$
$$\frac{\partial C_m}{\partial q} = \frac{-PM}{q^2 Sc}$$

The systematic standard uncertainty in C_m may be found as:

$$b_{C_m} = \left[\left(\frac{\partial C_m}{\partial PM} b_{PM}\right)^2 + \left(\frac{\partial C_m}{\partial q} b_q\right)^2\right]^{\frac{1}{2}}$$

Table A-2. Systematic Standard Uncertainty Estimates (*b*) for New Semi-span Balance using Representative Semi-span Icing Model

Description	Symbol	Nominal	Units	*b* (1 Std Dev)	Comments
Axial	*A*	–40	lbs	0.4	Stated at 0.08% of FS = 1000*
Normal	*N*	600	lbs	1.5	Stated at 0.03% of FS = 10000*
Pitching moment	*PM*	–62.5	ft-lbs	3.75	Stated at 0.05% of FS = 7500*
AOA	α	12	deg	0.035	*From similar NASA LaRC balance calibrations from turntable survey, performed in this study
Dynamic pressure	*q*	100.8	psf	0.0101	No uncertainty given, chosen as representative
Wing planform area	*S*	5.8	ft^2	const	
Chord	*c*	1.28889	ft	const	

Drag			Lift			Pitching Moment		
Partial Deriv		(b*PD)^2	Partial Deriv		(b*PD)^2	Partial Deriv		(b*PD)^2
dCD/dA =	0.0016731	4.4787E-07	dCL/dA =	-0.0003556	2.02349E-08	-	-	-
dCD/dN =	0.0003556	2.84553E-07	dCL/dN =	0.0016731	6.29817E-06	-	-	-
-		-	-		-	dCm/dPM =	0.0013271	6.19148E-06
dCD/dalpha =	1.0180710	3.86765E-07	dCL/dalpha =	-0.1464510	8.00342E-09	-	-	-
dCD/dq =	-0.0014529	2.14479E-10	dCL/dq =	-0.0100999	1.03647E-08	dCm/dq =	0.0008228	6.87942E-11

Appendix B. Calibration and Operation of the Force Balance System in the NASA-Glenn 6-ft by 9-ft Icing Research Tunnel

OVERVIEW OF THE IRT FORCE BALANCE SYSTEM

System Configuration

The test section of the IRT is 6 ft high, 9 ft wide, and 20 ft long. Centered in the floor of the test section is a model support turntable 8.8-ft in diameter. Referring to **Figure 1**, airfoil models are mounted vertically on the turntable, to be placed at required angles-of-attack to the airflow in the tunnel. When quantitative airload data are needed, for example to determine the effect of icing on the lift and drag characteristics of an airfoil, the IRT Force Balance System can be installed to provide test engineers with the ability to measure changes in airloads under icing conditions.

As shown schematically in Figure 1, components of the IRT Force Balance System are located below the turntable and in the tunnel ceiling above it. The system consists of lower and upper balances connected by a test model or (for calibration purposes only) by a vertical post to which a series of known horizontal loads are applied. A Calibration Rig, containing five hydraulic actuators and load cells, is installed temporarily in the test section to apply and measure these loads. The configuration of the Calibration Rig is described in the next section.

In the Force Balance System, the lower or "platform" balance is supported by a rigid outer structure that is connected to and rotates with the turntable, whose bearings and drive gears transfer lower-balance reactions to the tunnel structure and to ground. The top of the inner support structure (sometimes referred to as the "torque box") is connected rigidly to the test article, and the bottom is connected to a platform that is supported by legs with flexible sections. These permit the platform to move slightly in a horizontal plane, in response to airloads on the test article. The inner structure does not touch the turntable, so no airloads are transferred directly to the turntable.

Load cells RA, RB, and RC in the Force Balance measure the lower reactions to airloads. Using the chordline of the test model as a reference direction, Figure 1 shows that load cell RA measures the chordwise load applied to the platform, while load cells RB and RC measure load components normal to the chordwise direction. Because the lines of action of load cells RB and RC are 1.5 ft forward and aft of the vertical centerline of the turntable, the difference in their readings can be used to calculate the pitch moment load applied to the platform about a vertical axis. Because the outer support structure of the lower balance is fixed to the turntable, the orientations of the load cells remain chordwise and normal for all angles of attack.

The upper balance is wheel-shaped, with the test model (or calibration post) attached to the hub. Four spokes instrumented with strain gages connect the hub to the rim of the balance through flex plates. The rim is mounted in bearings that react lateral loads to ground, but do not react pitch moment loads. The strain gages on the spokes form load cells RD and RE for measuring normal and chordwise loads, respectively. The upper load cells also rotate with the test model, so the force components measured are always chordwise and normal for all angles of attack.

A pivot bearing connects the test model to the hub of the upper balance, which permits the upper end of a test model to rotate about any horizontal axis. Thus, when a model or calibration post is attached rigidly to the lower and by a pivot to the upper balance, its structural configuration is that of a propped cantilever. As a result, approximately 65% of lateral airloads on the model are transferred to the lower balance and 35% to the upper balance. All pitch moment loads are transferred to the lower balance. A test model can be supported by the lower balance only, in which case calibration of the force balance is performed with the post attached only at the bottom.

Photographs attached in **Appendix A** show views of various components of the force balance system.

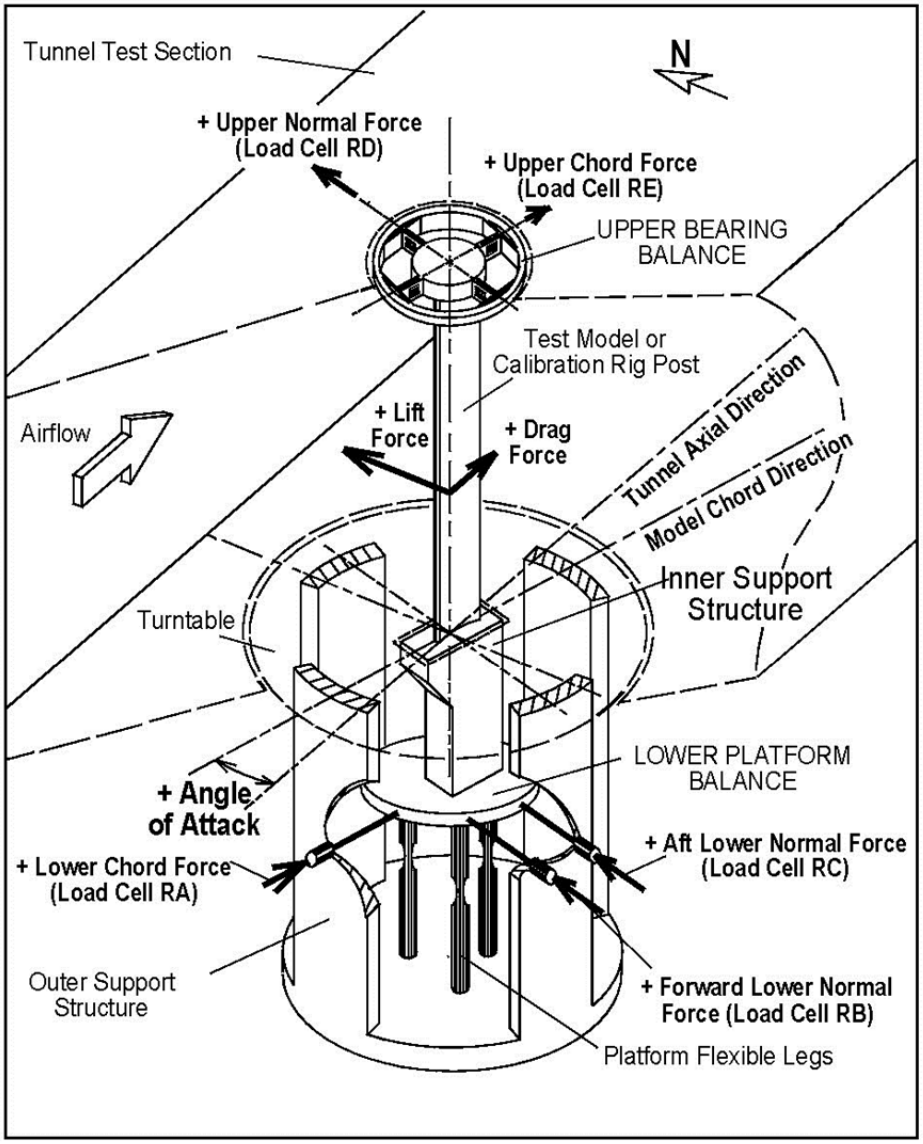

Figure 1. Schematic drawing of the Force Balance System in the Icing Research Tunnel. The main subassemblies are (1) a lower platform balance suspended from the model turntable and containing three load cells, and (2) an upper bearing balance mounted in the ceiling of the Test Section. Subassemblies rotate with the turntable, so measured loads are always along chordwise and normal axes with respect to the test article.

3

Force Balance Load Cell Capacities

Table 1 lists the capacities of the load cells in the Force Balance System. To increase measurement accuracy, the upper bearing balances are available in three load ranges: low, medium, and high. Because of the relatively low capacities of the chordwise load cells, special care must be taken during calibration and operation to avoid overloading the RA and any of the RE load cells. At non-zero angles of attack, chordwise loads on cells RA and RE can be significantly increased by vector components of the much larger lift forces. Therefore, loads on each cell are displayed by the ESCORT data system and should be monitored regularly.

Table 1. Capacities of Load Cells in the IRT Force Balance

Balance Location	Range	Cell Name	Serial Number	Load Direction	Capacity (lb)
Lower Platform	NA	RA	K710679	Chordwise	1,000
	NA	RB	702335	Forward Normal	5,000
	NA	RC	709569	Aft Normal	5,000
Upper Bearing	High	RD	M609156-Y	Normal	10,000
		RE	M609156-X	Chordwise	1,000
	Medium	RD	M616457-Y	Normal	2,000
		RE	M616457-X	Chordwise	500
	Low	RD	M616458-Y	Normal	3,700
		RE	M616458-X	Chordwise	120

Because cells RB and RC are separated 3.0 ft horizontally, the theoretical pitch moment capacity of the Force Balance is +/- 30,000 lb-ft, which is achieved when both RB and RC are at their force capacity of 10,000 lb but are oppositely directed.

OVERVIEW OF THE FORCE BALANCE CALIBRATION RIG

Rig Configuration

Each of the five load cells in the force balance, RA to RE, is first calibrated individually under laboratory conditions to determine its electrical output as a function of applied load. These results are expressed in millivolts of cell output per excitation volt per pound of load. However, when these load cells are installed in the force balance, secondary effects such as misalignment and friction can cause minor changes in the calibration. To account for these changes, the electrical outputs from all five load cells as-installed must be measured simultaneously while known loads are applied to a simulated test article mounted in the force balance. In 2000 a calibration rig was designed and fabricated so that the required large calibration forces could be applied safely and accurately to the force balance over a range of turntable angles of attack. The configuration of this rig is illustrated in **Figures 2 and 3,** and described in this section. The actual calibration procedure is described in a later section.

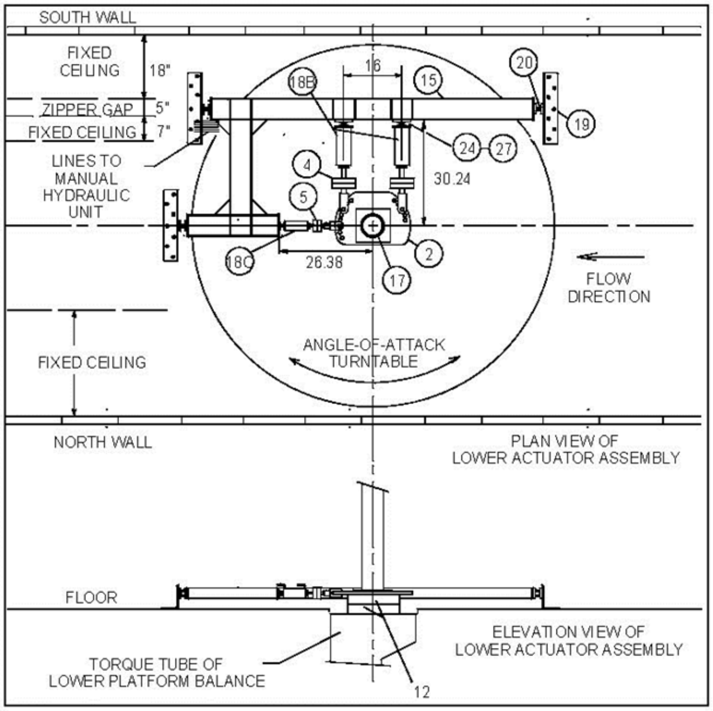

(a) General views

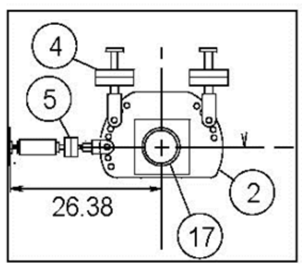

(b) Loading plate detail

Figure 2. Diagram of the lower actuator assembly of the Calibration Rig. Hydraulic actuators (18B) and (18C) with load cells (4) and (5) is connected individually to the loading plate (2) after the turntable rotates the connecting post (17) to the desired angle of attack. Support frame (15) is fastened to the tunnel floor and not to the turntable, so applied forces simulate lift and drag airloads at all angles of attack (circled numbers are part numbers).

As shown in Figures 2 and 3, the Calibration Rig is composed of lower and upper units, bolted to the floor and to the ceiling of the test section, respectively. Because the lower unit is not fastened to the turntable, its applied loads are always parallel and perpendicular to the tunnel axial direction. Thus, these applied loads represent lift and drag airloads at all angles of attack of the turntable. The same is true for loads applied with the upper actuators. Photographs in **Appendix B** show overall and close-up views of the Calibration Rig installed in the IRT test section. Manual pumps are used to supply hydraulic pressure to the calibration actuators.

The Calibration Rig is designed to permit calibration of the load cells in the force balance at five specific turntable angles of attack, namely 0 deg, +/- 10 deg, and +/- 20 deg. Referring to the loading plates designated as Parts 2 and 3 in Figures 2(b) and 3(b), all actuators are disconnected from these loading plates and the turntable is rotated to the selected angle of attack. Each actuator is then re-connected individually at the appropriate point on its loading plate. A series of loads is applied with only one actuator attached, and the output signals from all five of the load cells in the force balance are recorded in the ESCORT data system at each level of loading. The rig actuator is then disconnected from its loading plate. This process is repeated with all five actuators in the calibration rig. If required, the turntable is re-positioned at a different angle of attack and the load application sequence is repeated, again with only one rig actuator connected at a time.

Calibration Rig Load Cell Capacities

Table 2 lists the capacities of the five load cells in the Calibration Rig, designated Cal1 to Cal5. As noted previously, because of the relatively low capacities of the chordwise and drag load cells, special care must be taken during calibration and operation to avoid overloading load cells Cal1, Cal5, RA, and RE. At non-zero angles of attack, chordwise loads on cells RA and RE can be significantly increased by vector components of the much larger lift forces. Therefore, loads on each cell are displayed by the ESCORT data system and should be monitored regularly.

Table 2. Capacities of Load Cells in the Calibration Rig

Balance Location	Actuator Part Number	Actuator Number	Load Cell Number	Load Cell Serial Number	Load Direction	Capacity (lb)
Lower Unit	18C	1	Cal1	787992	Drag (+ East)	1,000
	18B	2	Cal2	778509	Forward Lift (+ North)	10,000
	18B	3	Cal3	812833	Aft Lift (+ North)	10,000
Upper Unit	18B1	4	Cal4	812834	Lift (+ North)	10,000
	18C	5	Cal5	786977	Drag (+ East)	1,000

Because cells Cal2 and Cal3 are separated 1.33 ft horizontally, the theoretical pitch moment capacity of the Calibration Rig is +/- 13,300 lb-ft, which is achieved when both Actuator 2 and Actuator 3 are at their force capacity of 10,000 lb but are oppositely directed.

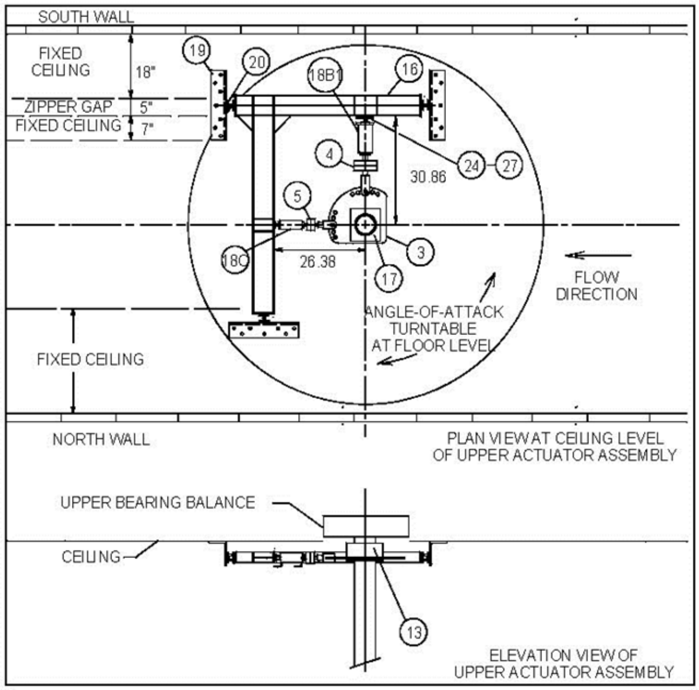

(a) General views

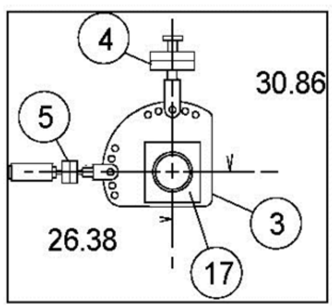

(b) Loading plate detail

Figure 3. Diagram of the upper actuator assembly of the Calibration Rig. After the connecting post (17) is rotated to the desired angle of attack, each of the hydraulic actuators (18B1) and (18C) with load cells (4) and (5) is connected individually to the loading plate (3) by a clevis and pin. Support frame (16) is fastened to tunnel ceiling, so applied forces simulate lift and drag airloads at all angles of attack (circled numbers are part numbers).

7

PROCEDURE FOR CALIBRATING THE FORCE BALANCE SYSTEM

Steps in the Calibration Procedure

Step 1. In the calibration laboratory, measure the signal gain of each of the five Force Balance load cells, RA to RE, and the five Calibration Rig load cells, Cal1 to Cal5. Signal gain is the slope of a line-fit of a graph of signal output *vs* applied load, expressed in millivolts per pound.

Step 2. Install the lower and upper units of the Calibration Rig in the Test Section, as illustrated in Figures 2 and 3.

Step 3. Set up the amplification ratios of 10 signal amplifiers: Five for signals from the Force Balance load cells RA to RE, and five for signals from the Calibration Rig load cells, Cal1 to Cal5. Use attached EXCEL spreadsheet "FBS AMP SETUP.xls" to calculate amplification ratios and the 30 reference calibration coefficients L1 to L10, D1 to D10, and M1 to M10, entering the signal gains from Step 1.

Step 4. Rotate the turntable to an angle of attack selected from the following: 0 deg, +/- 10 deg, or +/- 20 deg.

Step 5. Apply a specified sequence of lift and drag loads to the Force Balance using the actuators on the Calibration Rig one at a time, and simultaneously record in ESCORT at each load level the signal outputs from the five load cells in the Force Balance and the loads applied by the Calibration Rig.

Step 6. As required for additional angles of attack, repeat steps 4 and 5.

Step 7. Calculate a matrix of 15 calibration coefficients L1 to L5, D1 to D5, and M1 to M5 for each angle of attack. Equations for these calculations are derived in **Appendix D**.

Step 8. Remove the Calibration Rig from the tunnel.

Details of Steps 3, 5, and 7 are described below.

Step 3. Setup of Amplifiers

Setup of the 10 signal amplifiers consists of calculating and applying a custom amplification ratio to each, so that the selected full-scale output of each load cell in millivolts will be converted into the selected full-scale reading in engineering units. Entering sets of parameters (Part 4) into the ESCORT data system for converting cell outputs in millivolts to engineering units is also part of the setup process.

Setup calculations are performed using the attached Excel file "FBS AMP SETUP.xls". This file contains two template worksheets: FBSCELLS for the five load cells in the Force Balance System and CALRCELLS for the five load cells in the Calibration Rig. In addition, two sample spreadsheets are included with data for the June 2005 calibration of the Force Balance System.

The 30 calculated parameters L1 to L10, D1 to D10, and M1 to M10 are then entered into the appropriate ESCORT files.

Step 5. Apply Calibration Loads

With the turntable at a selected angle of attack, determine the maximum allowable load for each actuator by slowly applying hydraulic pressure to each actuator in turn and monitoring the output of each load cell in the Force Balance and Calibration Rig, with particular attention to chordwise and drag cells RA, RE, Cal1, and Cal5. <u>Care must be taken so that the capacity limits of these sensitive load cells are not exceeded.</u> For example, at angles of attack of +/- 20 deg, the

8

allowable loads applied by lift actuators 2, 3, and 5 may be decreased significantly, compared to allowable loads at a zero angle of attack. This is because of the increased size of the chordwise components of applied lift loads. Record these maximum allowable loads as F1max to F5max, for Calibration Rig actuators 1 to 5, respectively.

Next, with each of the five actuators in the Calibration Rig acting alone, apply a sequence of calibration loads in accordance with the list of loads in **Table 3**. Load steps in Table 3 are expressed as fractions of the maximum allowable load for that actuator and angle of attack. At each load step, record in an ESCORT file the five applied loads and the five outputs of the Force Balance load cells.

Step 7. Calculate a Matrix of Calibration Coefficients

Access **Appendix E**, the EXCEL workbook "IRT FBS CAL COEF.xls". Transfer the applied load and load cell output data (recorded in Step 6) from ESCORT to the "As-Measured Data" worksheet in this program, as explained in **Appendix F**. Successive worksheets for each angle of attack are linked to the as-measured data for the automatic calculation of the 15 calibration coefficients L1 to L5, D1 to D5, and M1 to M5. Measured lift forces, drag forces, and pitching moments are automatically calculated for each load step using these calibration coefficients. These measured loads are compared with the applied loads to evaluate the accuracy of the calibration. Variations between measured and applied loads are expressed as a percent of the maximum applied load. Graphs are also provided in which measured loads are plotted versus applied loads, with trend lines and equations.

The final worksheet in this workbook is "Summary", which lists the 15 calibration coefficients calculated for each of the angles of attack. This listing of coefficients will be carried forward to the workbook used for post-processing of the airload test data.

Note: It is not necessary to change any of the reference parameters in ESCORT (entered in Step 5) after completing the calibration process. These reference parameters are sufficiently accurate for monitoring airloads as displayed on the ESCORT screens.

PROCEDURE FOR PROCESSING AIRLOAD TEST DATA FROM THE FORCE BALANCE SYSTEM

The IRT Force Balance System is designed to measure the effects of icing on the lift, drag, and pitching moment coefficients of a test airfoil, as functions of angle of attack and airspeed. The procedure for making these measurements is illustrated in **Appendix G**, which is the EXCEL workbook "SAMPLE AIRLOAD TEST.xls". The first worksheet in this program is a copy of the "Summary" worksheet in the workbook "IRT FBS CAL COEF.xls", which makes the calibration coefficients readily available for post-processing of the test airload data.

The first step in measuring the airload characteristics of the test model is to record in ESCORT a set of zero readings from the five load cells in the Force Balance. The tunnel fan must be off (or at a very low speed) for these zero readings, but the tunnel should be at or near the selected test temperature. If possible, a zero data point is taken at each angle of attack planned for the actual airload test. If this is not possible, interpolation can be used to calculate zero readings for other test angles of attack. The angles of attack and related zero readings, designated as RA0 to RE0, are then transferred to the EXCEL worksheet "Zero Runs". Graphs of the zero readings versus angle of attack are provided in the program, for monitoring trends.

Table 3. Sequence of Applied Calibration Loads

Applied load step	Forces applied with Calibration Rig actuators Fi,max = max allowable load at selected angle of attack on actuator i, i = 1 to 5 No entry = actuator disconnected				
	F1 + = East	**F2** + = North	**F3** + = North	**F4** + = North	**F5** + = East
1	+ 0				
2	+ 0.33 F1,max				
3	+ 0.67 F1,max				
4	+ 1.00 F1,max				
5	+ 0.50 F1,max				
6	+ 0				
7		- 0			
8		- 0.33 F2,max			
9		- 0.67 F2,max			
10		- 1.00 F2,max			
11		- 0.50 F2,max			
12		- 0			
13		+ 0			
14		+ 0.33 F2,max			
15		+ 0.67 F2,max			
16		+ 1.00 F2,max			
17		+ 0.50 F2,max			
18		+ 0			
19			- 0		
20			- 0.33 F3,max		
21			- 0.67 F3,max		
22			- 1.00 F3,max		
23			- 0.50 F3,max		
24			- 0		
25			+ 0		
26			+ 0.33 F3,max		
27			+ 0.67 F3, max		
28			+ 1.00 F3, max		
29			+ 0.50 F3, max		
30			+ 0		
31				- 0	
32				- 0.33 F4, max	
33				- 0.67 F4, max	
34				- 1.00 F4, max	
35				- 0.50 F4, max	
36				- 0	
37				+ 0	
38				+ 0.33 F4, max	
39				+ 0.67 F4, max	
40				+ 1.00 F4, max	
41				+ 0.50 F4, max	
42				+ 0	
43					+ 0
44					+ 0.33 F5, max
45					+ 0.67 F5, max
46					+ 1.00 F5, max
47					+ 0.50 F5, max
48					+ 0

10

As shown in the sample data set, zero runs (numbered 13, 15, and 17) were made before and after each test run (numbered 14 and 16), and the load cell readings from two zero runs were averaged and then used to correct the appropriate test run data.

Test runs at different airspeeds (175 kt and 130 kt for Run Nos. 14 and 16, respectively) are then conducted over a range of angles of attack, and load cell readings are recorded in ESCORT. These readings are then transferred to the appropriate worksheets in this EXCEL workbook. Zero corrections are then made automatically to the measured load cell outputs.

The data analyst must then copy the calibration angles of attack and related calibration coefficients from the "Summary" worksheet to each test run worksheet, locating them on lines appropriate for interpolation. In the samples, the copied calibration data are in bold print, while the interpolated coefficients are not. This results in a set of 15 calibration constants for every angle of attack at which test data were taken. Again, it is not necessary to change the reference parameters entered into ESCORT as part of the amplifier setup process.

The remainder of the airload performance parameters is now calculated automatically, including the following: Normal, chordwise, lift, and drag forces; pitching moments about the turntable centerline and about the 1/4-chord axis of the airfoil; lift, drag, and moment coefficients; and wall effect corrections to these coefficients and the angle of attack. Samples of graphs are provided that display lift, drag, and moment coefficients versus angle of attack, with all data corrected for wall effects.

This completes the processing of the readings from the Force Balance to obtain airload performance parameters.

APPENDIX F

TRANSFER OF DATA FROM ESCORT TO EXCEL WORKSHEET

ESCORT Batch Procedure

A sample of the transferred data is displayed in **Appendix H**. The transfer procedure is as follows:

1. Open a new window on the ESCORT terminal and select the program to be batched.
2. Type EB at the prompt.
3. Select **1 - Process some data**.
4. Enter the reading numbers "# - ###".
5. Select the output option **- 111, 112, 113, …** for the desired number of data files.
6. Type "/" to quit.
7. Log out of the open window.
8. Log onto the ESCORT PC.
9. Select the FTP icon.
10. Select the correct source and destination directories.
11. Verify ASCII is selected.
12. Move the proper data files from the ESCORT computer to the ESCORT PC.
13. Close the FTP application.
14. Navigate to the destination directory.
15. Open DATA01, DATA02,…. using EXCEL (AU Files).
16. Using the COPY MOVE SHEET commands merge all data sheets into one workbook. Rename each sheet with the proper nomenclature.
17. Set the column width to 12 on all worksheets.
18. Save the merged file as a MS EXCEL Workbook with the following nomenclature:

    D0##ABCDEFG_MMDDYY

where

D0## = program number

ABCDEFG = program name

MMDDYY = run date

19. Check the saved file for data fullness and data accuracy.

Appendix C. Turntable Measurement Data

Table C-1. Unidirectional Positive to Negative[2]

True Angle	Set Point	Set Point Error	Feedback	Feedback Error
18.43	18.50	0.07	18.41	−0.02
16.94	17.00	0.06	16.91	−0.03
14.95	15.00	0.05	14.91	−0.04
12.97	13.00	0.03	12.91	−0.06
10.97	11.00	0.03	10.91	−0.06
9.00	9.00	0.00	8.92	−0.08
6.99	7.00	0.01	6.92	−0.07
4.99	5.00	0.01	4.91	−0.08
3.99	4.00	0.01	3.91	−0.08
3.00	3.00	0.00	2.91	−0.09
2.00	2.00	0.00	1.91	−0.09
1.50	1.50	0.00	1.41	−0.09
1.01	1.00	−0.01	0.92	−0.09
0.50	0.50	0.00	0.40	−0.10
0.00	0.00	0.00	−0.08	−0.08
−0.49	−0.50	−0.01	−0.58	−0.09
−0.98	−1.00	−0.02	−1.08	−0.10
−1.49	−1.50	−0.01	−1.58	−0.09
−1.99	−2.00	−0.01	−2.08	−0.09
−2.98	−3.00	−0.02	−3.08	−0.10
−3.98	−4.00	−0.03	−4.08	−0.11
−4.98	−5.00	−0.02	−5.08	−0.10
−6.97	−7.00	−0.03	−7.08	−0.11
−8.95	−9.00	−0.05	−9.08	−0.13
−10.94	−11.00	−0.06	−11.08	−0.14
−12.95	−13.00	−0.05	−13.08	−0.13
−14.93	−15.00	−0.07	−15.08	−0.15
−16.93	−17.00	−0.07	−17.08	−0.15
−18.91	−19.00	−0.09	−19.08	−0.17

[2] True Angle - the true angle of the turntable as read by the Theodolite.
Set Point - Position angle commanded by the wind tunnel control system.
Set Point Error - difference between the set point and true angle.
Feedback - the encoder reading of the position of the turntable.
Feedback error - the difference between the encoder reading and true angle.

Table C-2. Unidirectional Negative to Positive[3]

True Angle	Set Point	Set Point Error	Feedback	Feedback Error
–18.43	–18.50	–0.07	–18.58	–0.15
–16.94	–17.00	–0.06	–17.09	–0.15
–14.95	–15.00	–0.05	–15.09	–0.14
–12.98	–13.00	–0.02	–13.10	–0.12
–10.99	–11.00	–0.01	–11.10	–0.11
–9.00	–9.00	0.00	–9.09	–0.09
–7.00	–7.00	0.00	–7.09	–0.09
–5.02	–5.00	0.02	–5.09	–0.08
–4.02	–4.00	0.02	–4.09	–0.07
–3.01	–3.00	0.01	–3.10	–0.09
–2.01	–2.00	0.01	–2.10	–0.09
–1.52	–1.50	0.02	–1.59	–0.07
–1.02	–1.00	0.02	–1.10	–0.08
–0.51	–0.50	0.01	–0.59	–0.08
0.00	0.00	0.00	–0.08	–0.08
0.48	0.50	0.02	0.41	–0.07
0.98	1.00	0.02	0.90	–0.08
1.49	1.50	0.01	1.40	–0.09
1.98	2.00	0.02	1.90	–0.08
2.99	3.00	0.02	2.90	–0.09
3.98	4.00	0.02	3.90	–0.08
4.98	5.00	0.02	4.91	–0.07
6.97	7.00	0.03	6.91	–0.06
8.96	9.00	0.04	8.90	–0.06
10.95	11.00	0.05	10.90	–0.05
12.95	13.00	0.05	12.90	–0.05
14.94	15.00	0.06	14.90	–0.04
16.93	17.00	0.07	16.90	–0.03
18.91	19.00	0.09	18.90	–0.01

[3]True Angle - the true angle of the turntable as read by the Theodolite.
Set Point - Position angle commanded by the wind tunnel control system.
Set Point Error - difference between the set point and true angle.
Feedback - the encoder reading of the position of the turntable.
Feedback error - the difference between the encoder reading and true angle.

Table C-3. Random Run[4]

True Angle	Set Point	Set Point Error	Feedback	Feedback Error
0.00	0.00	0.00	–0.09	–0.09
–18.91	–19.00	–0.09	–19.09	–0.18
0.00	0.00	0.00	–0.08	–0.08
18.91	19.00	0.09	18.90	–0.01
0.00	0.00	0.00	–0.08	–0.08
–14.95	–15.00	–0.05	–15.09	–0.14
–0.01	0.00	0.01	–0.08	–0.07
14.94	15.00	0.06	14.90	–0.04
0.00	0.00	0.00	–0.08	–0.08
–9.96	–10.00	–0.04	–10.08	–0.12
–0.01	0.00	0.01	–0.09	–0.08
9.96	10.00	0.04	9.91	–0.05
–0.01	0.00	0.01	–0.08	–0.07
–6.98	–7.00	–0.02	–7.08	–0.10
–0.01	0.00	0.01	–0.09	–0.08
6.97	7.00	0.03	6.91	–0.06
–0.01	0.00	0.01	–0.09	–0.08
–4.99	–5.00	–0.01	–5.09	–0.10
–0.01	0.00	0.01	–0.09	–0.08
4.98	5.00	0.02	4.91	–0.07
–0.01	0.00	0.01	–0.08	–0.07
–2.00	–2.00	0.00	–2.08	–0.08
0.00	0.00	0.00	–0.07	–0.07
1.99	2.00	0.01	1.90	–0.09
–0.01	0.00	0.01	–0.09	–0.08
–1.01	–1.00	0.01	–1.09	–0.08
0.00	0.00	0.00	–0.07	–0.07
0.98	1.00	0.02	0.91	–0.07
–0.01	0.00	0.01	–0.08	–0.07
1.98	2.00	0.02	1.90	–0.08
–2.00	–2.00	0.00	–2.08	–0.08
4.98	5.00	0.02	4.90	–0.08
–4.99	–5.00	–0.01	–5.09	–0.10
9.96	10.00	0.04	9.91	–0.05
–9.96	–10.00	–0.04	–10.08	–0.12
17.93	18.00	0.07	17.91	–0.02
–17.94	–18.00	–0.06	–18.08	–0.14
–0.01	0.00	0.01	–0.09	–0.08

[4] True Angle - the true angle of the turntable as read by the Theodolite.
Set Point - Position angle commanded by the wind tunnel control system.
Set Point Error - difference between the set point and true angle.
Feedback - the encoder reading of the position of the turntable.
Feedback error - the difference between the encoder reading and true angle.

REPORT DOCUMENTATION PAGE	*Form Approved* *OMB No. 0704-0188*

1. REPORT DATE *(DD-MM-YYYY)*	**2. REPORT TYPE**	**3. DATES COVERED** *(From - To)*
01- 11 - 2012	Technical Memorandum	July 2010 - October 2012

4. TITLE AND SUBTITLE Icing Research Tunnel (IRT) Force Measurement System (FMS)	**5a. CONTRACT NUMBER**
	5b. GRANT NUMBER
	5c. PROGRAM ELEMENT NUMBER
6. AUTHOR(S) Roberts, Paul W.	**5d. PROJECT NUMBER**
	5e. TASK NUMBER
	5f. WORK UNIT NUMBER 869021.05.07.08.01
7. PERFORMING ORGANIZATION NAME(S) AND ADDRESS(ES) NASA Langley Research Center Hampton, VA 23681-2199	**8. PERFORMING ORGANIZATION REPORT NUMBER** L-20207 NESC-RP-10-00632
9. SPONSORING/MONITORING AGENCY NAME(S) AND ADDRESS(ES) National Aeronautics and Space Administration Washington, DC 20546-0001	**10. SPONSOR/MONITOR'S ACRONYM(S)** NASA
	11. SPONSOR/MONITOR'S REPORT NUMBER(S) NASA/TM-2012-217784

12. DISTRIBUTION/AVAILABILITY STATEMENT
Unclassified - Unlimited
Subject Category - 09 Research and Support Facilities (Air)
Availability: NASA CASI (443) 757-5802

13. SUPPLEMENTARY NOTES

14. ABSTRACT

An Electronics Engineer at the Glenn Research Center (GRC), requested the NASA Engineering and Safety Center (NESC) provide technical support for an evaluation of the existing force measurement system (FMS) at the GRC's Icing Research Tunnel (IRT) with the intent of developing conceptual designs to improve the tunnel's force measurement capability in order to better meet test customer needs. This report contains the outcome of the NESC technical review.

15. SUBJECT TERMS
NASA Engineering and Safety Center; Force measurement system; Icing Research Tunnel; Wind tunnel

16. SECURITY CLASSIFICATION OF:			**17. LIMITATION OF ABSTRACT**	**18. NUMBER OF PAGES**	**19a. NAME OF RESPONSIBLE PERSON**
a. REPORT	**b. ABSTRACT**	**c. THIS PAGE**			STI Help Desk (email: help@sti.nasa.gov)
					19b. TELEPHONE NUMBER ***(Include area code)***
U	U	U	UU	73	(443) 757-5802